ENGINEERING RESEARCH INSTITUTE
DEPARTMENT OF AERONAUTICAL ENGINEERING
UNIVERSITY OF MICHIGAN

A STUDY OF THE COMPUTER SECTION OF FLIGHT SIMULATORS

Department of the Air Force
Contract No. AF 33(616)-21B1
E. O. No. R668-421 PO-3a

FINAL REPORT

March, 1954

Project 2164

Submitted for the project by:

R. M. Howe

J. D. Schetzer

TABLE OF CONTENTS

TABLE OF CONTENTS (cont.)

TABLE OF CONTENTS (cont.)

TABLE OF CONTENTS (cont.)

LIST OF ILLUSTRATIONS

PERSONNEL EMPLOYED ON THIS PROJECT

F. L. Bartman	Research Engineer	
J. E. Broadwell	Assistant Professor	
E. G. Gilbert	Instructor	
E. O. Gilbert	Instructor	
V. S. Haneman	Captain USAF	
L. M. Harrison	Secretary	
H. F. Henry	Research Technician	
R. M. Howe	Assistant Professor	Supervisor
J. A. Lauder	Research Technician	
R. E. Peck	Research Technician	
J. W. Peterson	Assistant in Research	
L. L. Rauch	Professor	
J. D. Schetzer	Professor	

Note:

Captain V. S. Haneman, Jr. is a USAFIT student officer at the University of Michigan as a Ph.D. applicant and is working on this project as part of his doctoral thesis.

CHAPTER 1

INTRODUCTION

1.1 Scope of the Study Program

This report summarizes the results of a nine-month study of the computer section of flight simulators used for training aircraft crews. Simulators of this type consist of a complete mock-up of the aircraft cockpit, a trouble console which allows the instructor to introduce various simulated malfunctions, and a computer which solves the aircraft flight equations and displays the results on the cockpit instruments. The present Air Force simulators are exhibiting excellent utility in training crews of bomber, fighter, and transport aircraft. Even more extensive use of this type of training device is anticipated in the future. However, the present simulators do require considerable maintenance, large amounts of electrical power, and often exhibit inadequate dynamic characteristics. With a view to improving the above difficulties by changing the methods of electronic computation or possibly by some standardization in the computer section, the present study program was initiated.

This program has fallen roughly into three parts; (1) a study of methods of computation used by the simulator manufacturers and by the computer industry in general; (2) a study of the flight equations used by the simulator manufacturers, the airframe manufacturers, and the guided-missile industry; (3) a study of the performance of the trainers at the various bases, including engineering tests, study of maintenance problems, pilot complaints, etc.

This report discusses the results of the investigations mentioned above and presents a number of specific recommendations for the computer sections of future training-type simulators (see Section 1.3). These recommendations are based on our own background in the computer field and on discussions with the groups contacted in the course of this project. In many cases they are recommendations which have for some time been carried out in simulators outside the aircraft-trainer industry. Also some of the simulator manufacturers may agree with the recommendations but do not have the research and development funds necessary to implement them.

1.2 Summary of the Study Program

In order to give the reader an idea of the basis for the overall study program, we have summarized below the places which were visited and the investigations which were made with our own computing facility.

1.2.1 Visits to Simulator Manufacturers. The simulator manufacturers listed below were visited at least once and in some cases twice in order to discuss the engineering aspects of their trainers, particularly the computer sections.

Curtiss Wright Corporation, Carlstadt, New Jersey
Engineering and Research Corporation, Riverdale, Maryland
Goodyear Aircraft Corporation, Akron, Ohio
Link Aviation, Inc., Binghamton, New York
Melpar, Inc., Alexandria, Virginia
Union Switch and Signal Company, Pittsburg, Pennsylvania

1.2.2 Visits to Computer Manufacturers. The following companies were visited to discuss commercial analog computer developments.

Electronic Associates, Inc., Long Branch, New Jersey
Goodyear Aircraft Corporation, Akron, Ohio

1.2.3 Visits to Air Force and Navy Bases. These bases were visited to discuss simulator installations and where indicated to conduct actual performance tests on the trainers. In the case of Special Devices Center, the visit was for the purpose of discussing simulator and computer programs of the Navy.

Hunter Air Force Base, Savannah, Georgia (B-50 trainer)
Macdill Air Force Base, Tampa, Florida (tests on B-47 trainer)
MATS, West Palm Beach, Florida (tests on C-124A trainer)
Navy Special Devices Center, Sands Point, Long Island, New York
Peron Air Force Base, Dennison, Texas (F-86D trainers)
Tyndall Air Force Base, Panama City, Florida (tests on F-86D trainer)

1.2.4 Visits to Aircraft Companies. Aircraft companies visited include those on the following list. These visits were to discuss simulation activities at the companies, accuracy of aerodynamic terms, aircraft performance, etc.

Consolidated Vultee Aircraft Corporation (Convair), San Diego, California
Consolidated Vultee Aircraft Corporation (Convair), Forth Worth, Texas
Douglas Aircraft Company, Inc., Long Beach, California
Douglas Aircraft Company, Inc., Santa Monica, California
Hughes Aircraft Company, Culver City, Colorado
North American Aviation, Inc., Inglewood, California
Northrup Aircraft, Inc., Hawthorne, California

1.2.5 Solution of the F-86D Equations. In order to study the accuracy possibilities of dynamic simulation and possible mechanizations of equations, portions of the F-86D flight equations were set up and solved on the dc electronic differential analyzer facility of the Department of Aeronautical Engineering, University of Michigan. Results were compared with North American calculations, ERCO trainer performance, and actual flight-test data.

In addition, a visit to the Moore School of Electrical Engineering, University of Pennsylvania, was made to discuss with Dr. Morris Rubinoff their work for the Navy on the use of digital computers for aircraft simulation.

1.3 Recommendations as a Result of the Study Program

As a direct result of this study program a number of recommendations concerning the computer sections of future flight simulators can be made. These include not only recommendations regarding the type of electronic computing devices to be used but also suggestions which should improve the development time and costs, as well as effectiveness of future trainers. The entire list of recommendations appears here for the convenience of the reader; engineering support for the recommendations is contained in the bulk of the report.

(1) It is recommended that the present ac 60 cycle carrier analog computing systems in the trainers be replaced by dc analog systems in future trainers. The dc systems will exhibit greatly improved dynamic performance, decreased development time for each new trainer, decreased calibration and check-out time, more opportunity for built-in automatic checking devices, easier maintenance, and easier incorporation of modifications of the flight equations once the trainer is in the field. It should not be necessary to drift stabilize the bulk of the dc amplifiers in the computer.

(2) Centrally located power supplies, preferably of the motor-generator type, should be employed.

(3) For multiplication, servo-driven potentiometers still seem to be the most reliable and easily maintained arrangement. 400 cycle motors driven by magnetic amplifiers appear to be the best combination. Tapped potentiometers are recommended for function generation.

(4) It is recommended that self-testing circuits be incorporated in the computer section, circuits which will check amplifier balance, gain, and overall static performance of the computer. This is readily possible with a dc system, and the circuits can be designed so that

a failure in the testing device will not affect operation of the simulator.

(5) Stick forces should be provided by means of a torque-producing device employing feedback, such as a torque tube.

(6) Portions of the computer dealing with simulation of the fire-control system should not employ the actual GFE aircraft fire-control equipment, since the latter is not, in general, intended for continuous duty and does not have the advantage of many of the physical input data available in the trainer. A more reliable and satisfactory simulation of the fire-control problem can be mechanized in a portion of the computer section of the trainer.

(7) It is recommended that in the future a much closer liason between simulator and airframe manufacturer be maintained. This is particularly important where the airframe manufacturer is doing considerable simulation work himself as a design and analysis aid. Such liason should in all cases result in more accurate and up-to-date aircraft data being furnished to the simulator manufacturer.

(8) The dynamic flight equations, at least in linearized form, should be set up and solved on accurate analog computing equipment before a final computer mechanization for the trainer is decided upon. This is essential to determine the relative importance of various aerodynamic terms, which terms can be eliminated, importance of things like products of inertia, correlation with preliminary flight test data when available, possible errors in the data furnished by the airframe manufacturer, etc.

(9) Specifications on the performance of trainers should not, in general, include increased absolute accuracy but should be increased in comprehensiveness to include dynamic requirements, resolution requirements, and slope as well as magnitude requirements in such things as stick-force versus displacement simulation.

(10) It is recommended that support for research and development of digital computer sections for flight simulators be provided. Only by actual using experience with this type of computer and the many analog to digital and digital to analog conversions necessary for operation as a flight simulator will an ultimate comparison of the digital system will present or projected analog system be possible.

CHAPTER 2

SUMMARY OF THE FLIGHT EQUATIONS
PRESENT AND PROPOSED ELECTRONIC METHODS USED FOR THEIR SOLUTION

2.1 Brief Summary of the Flight Equations

The basic computational problem in the computer section of flight simulators involves the solution of equations which describe the position and angular orientation in space of a rigid body, namely the aircraft. These equations have as inputs the motion of the control stick, rudder pedals, engine controls, and other auxiliary devices, while the computed outputs such as airspeed, heading, attitude, rate of turn, altitude, engine rpm, etc., must be displayed on the cockpit instruments.

Essentially there are six dynamic equations which must be solved (see Appendix I). These are the equations of motion representing translation along three axes and rotation about three axes. Each of the three equations for translation has input forces along its particular axis, forces which result from aerodynamic, propulsive, or gravity terms. The forces in turn cause accelerations along each of the axes, and these accelerations must be integrated to provide the velocities along the translational axes. In the same way each of the three equations for rotation has input moments about its particular axis. These moments cause angular accelerations about the axes, accelerations which must be integrated to obtain the angular velocities. By performing certain trigonometric operations on the angular velocities and integrating the resulting velocities, the orientation angles of the aircraft with respect to the earth (bank, altitude, and heading angles) are obtained. These angles are in turn used to resolve the three translational velocities described earlier into velocities north, east, and vertical (rate of climb), which after integration yields the aircraft position and altitude.

Thus the solution of the flight equations involves summation, integration with respect to time, multiplication, and trigonometric resolution. In addition, the calculation of the aerodynamic translational forces and moments involves generation of arbitrary functions (e.g., functions of Mach number, altitude, etc.) and

division. Solution of the propulsion equations which give such outputs as thrust, rpm, etc., may involve function generation, integration, summation, and multiplication.

One of the important decisions which must be made when solving the flight equations is the selection of an axis system in which to perform the computation of the six equations of motion. The problem is made difficult by the fact that the aircraft does not fly in the direction in which it is pointed; but, in general, has an angle of attack α and an angle of sideslip β (see Appendix II). The coordinate system which has its X axis aligned with the direction in which the aircraft is moving is called the wind axes system, while the coordinate system which has its X axis aligned with the direction in which the aircraft is pointed (i.e., fixed to the aircraft) is called the body axis system. The wind axis system has the advantage that aerodynamic forces and moments are easily calculated, but it has the disadvantage that exact solution of the three rotational equations is extremely complicated. The body axis has the advantage of the simplest solution of the three rotational equations of motion but the disadvantage of a more complicated calculation for the aerodynamic forces and moments. Both systems involve equal complication for solution of the exact translational equations.

Another axis system which is used to define aerodynamic parameters is the stability axis system. This system differs from the body axis system by the angle of attack of the aircraft (see Appendix II).

2.2 Coordinate Systems Used by Simulator Manufacturers

It should be of some interest to mention the coordinate axes systems used by some of the simulator manufacturers. ERCO solves the six equations of motion in the body axes (e.g., the F-86D); this means that the Union Switch and Signal F-86D trainers also use the body axis system. In both cases the aerodynamic forces and moments are computed in the stability axes (see Appendix II) and are then resolved by small angle theory into the body axes. Link solves the equations of motion in the wind axes (e.g., the B-47), which means that many terms in the three rotational equations must be neglected (this, of course, may be justifiable). We have been unable to obtain sufficient information about the Curtiss Wright simulators to make a general statement concerning the coordinate axes systems in use.

All missile simulator installations with which we are familiar use the body axis system. It appears to us that, in general, this system is definitely the best for rotational equations, and is at least as good as a wind-axis system for the translational equations from the point of view of complexity. Further and more detailed study of this problem will be continued by the University of Michigan group.

2.3 Computation Methods Used by the Simulator Manufacturers; Advantages and Disadvantages

2.3.1 General. All of the training-type simulator manufacturers with the exception of Goodyear Aircraft are using 60 cycle supressed-carrier amplitude-modulated computing systems; Goodyear is using a 400 cycle system. In computers of this type the various dependent variables are represented by the amplitude of the ac carrier signal. Positive signals are distinguished from negative signals by reversed phase of the modulated signal relative to the carrier reference. In such ac systems the preservation of phase angle to zero or 180 degrees with respect to the carrier reference is important. However, stray capacitance in interconnecting leads, resistive computing components, etc., can cause serious phase shifts. For this reason it is important to keep the impedance of computing elements low, which for reasonable voltage levels means high currents and hence considerable power dissipation.

A disadvantage of the 60 cycle systems is the limited bandwidth available for the computing signals. Unless single side-band demodulation is used (this is not the case in practice) the absolute maximum frequency component which can be handled in the computation is 60 cps, whereas practically the limit is considerably below this. Despite the fact that present or projected aircraft have no natural frequencies in their dynamic behavior which are above several cycles per second, large errors in the spectral components of the order of 60 cps or higher may cause considerable deviation in computer response compared with the actual aircraft. The Goodyear 400 cps systems improve this situation but increase inaccuracy difficulties arising from stray capacitance.

Another disadvantage of ac carrier-modulated systems is the complexity required for elementary dynamic operations, such as integration, representation of simple time lags, etc. In most cases all-electronic circuits for simulation of these dynamic operations are complicated and are highly sensitive to shifts in the carrier frequency, which for 60 cycle systems usually means shifts in the line frequency of the local base power source. The obvious alternative, electromechanical devices for dynamic operations, has disadvantages which will be discussed for the case of integrators in 2.3.4).

2.3.2 Summers. All simulator manufacturers use ac amplifiers with considerable feedback for summation (see Appendix III). Essentially, the input ac voltages to be summed are applied through resistors to the input of the amplifier. The sum of the resulting currents through the input resistors flows through the feedback resistor and hence generates a voltage at the amplifier output proportional to the sum of the input voltages. Summation by means of this type of high-gain amplifier makes the performance of the summer virtually independant of such vacuum

tube characteristics as nonlinearities, small changes in amplification factor, etc. The ac amplifiers have the advantage of no zero-drift problem. In addition they have slightly fewer components than dc amplifiers and may therefore be somewhat more reliable. However, dc amplifiers can be made extremely reliable (our own experience as well as the experience of others confirms this) and with well regulated power supplies zero drift of the dc amplifiers is negligible for simulator applications. Chopper stabilized dc amplifiers can always be used in critical locations if any drift problems are encountered (see Appendix III).

2.3.3 Integrators. For ac carrier modulated computers the only practical integration technique involves the use of electromechanical integrators. These are essentially servos which, by means of ac tachometer feedback, generate a rate of output shaft rotation proportional to the input ac signal to be integrated. Thus the output shaft angle is proportional to the time integral of the input voltage. By means of a potentiometer on the output shaft the angle of shaft rotation can be converted back to an ac carrier-modulated voltage. Additional pots on the output shaft can be used to multiply the integrated signal by other voltages.

Since they use ac computers, all of the simulator manufacturers are utilizing the velocity-servo-type integrators. One advantage of this type of integrator is ease with which the integrated output can be multiplied by other variables, merely by adding multiplying potentiometers on the output shaft. However, the velocity-servo-type integrator has a number of serious disadvantages. One of the primary difficulties lies in the ac tachometers, which have a residual ac output voltage even when the tachometer shaft is stationary. This residual voltage may vary from one part in several hundred to, at very best, one part in several thousand when compared with the full scale output voltage of the tachometer. The result is very poor performance of the integrator for small signal inputs.

Another disadvantage of servo integrators is that the dynamics of the integrator response are limited by the servo dynamics. The resulting lags can cause important dynamic errors in simulating high-performance aircraft. Also, the ac voltage representing the integrated output must be obtained from the wiper-arm of a potentiometer driven by the output shaft; since the pots used by the simulator manufacturers have only from 1000 to 2000 wire turns, there is very appreciable granularity in the output voltage as the wiper-arm moves from wire to wire. This, too, can cause serious dynamic errors for small-amplitude aircraft motions, which is the type of motion involved in normal flight. Finally, nonlinearities in velocity-servo operation resulting from Coulomb friction in the servo will cause poor integrator operation with small signal inputs.

None of the above disadvantages cited for ac servo integrators are present in dc all-electronic integrators (see Appendix III). The only appreciable error in the dc integrators which might possibly effect their satisfactory operation is integrator drift due to unbalance in the dc amplifier. The latter can be

held easily to one part in 5,000 of full scale for manually balanced amplifiers. In any case the drift is a linear effect which does not affect the dynamics of the simulator for small motions. It only introduces effects equivalent to such things as very slight trim changes in the aircraft or wind of less than one knot. Where open ended integrations are required, such as in the computation of north and east position or altitude, drift-stabilized amplifiers can be used. These may easily be built to hold the drift referred to input to within one part in 1,000,000 of full scale.

There are probably several integrators in the computer section of the simulator which might have to be of the velocity-servo type, despite the fact that a dc system is employed. These would be the ones integrating bank and heading rates into bank and heading angles respectively. Here the angle outputs to the resolving servos must be periodic every 2π radians, and the simplest mechanization would appear to be a dc velocity servo. However, dc tachometers are several orders of magnitude better than ac tachometers with regard to full-scale to residual levels, and hence most of the small-motion errors in the ac integrators would not be present in the dc servo integrators.

2.3.4 Multiplication and Division. All of the simulator manufacturers perform multiplications in the computer by means of servo-driven potentiometers. Present systems employ two-phase amplifier-driven motors at the ac carrier frequency (60 cps except for Goodyear, which used 400 cps). In every case the multiplying pots have from 1000 to 2000 turns, which in some cases can result in granularity difficulties causing poor small-motion behavior, as described in the integrator discussion (2.3.4). Another disadvantage of servo multipliers is their slow dynamic response, which can cause important errors in simulating some of the high performance aircraft. Also, the servos require considerable power for operation.

If a dc computer is used, all electronic time-division multipliers can be used. Speed of response of such multipliers is several order of magnitude higher than that of the servo multiplier, and accuracy capabilities are similar. However, it is our feeling, after discussing servo and all-electronic multipliers with the analog computer industry, that the servo multipliers are definitely preferable if the dynamic lags are tolerable. This is because of the increased complexity (e.g., many more vacuum tubes) and more frequent adjustment required for the electronic multipliers. It is also our feeling that the speed of response and the reliability of the servo multipliers used currently by the simulator industry can be greatly increased with at the same time a reduction in power requirements. With a dc computer system this can be accomplished by using a standard dc computer amplifier (similar to those for summation and integration) driving a 400 cps magnetic amplifier, which in turn powers the variable phase of a high-performance, 2-phase 400 cycle servo motor.

Even using the limited bandwidth of 60 cycle amplifiers and motors we have tested servo multipliers with closed-loop natural frequencies of 25 cps and maximum response figures of 1000 volts/sec and 20,000 volts/sec^2 ($\pm$ 100 volts = full scale). These servos were driving 5 one-turn pots, each pot having 4500 turns. With 400 cps motors these response speeds can be further improved. Commercially available servo multipliers (e.g., Electronic Associates) also fall in this response range.

If there are several multiplications in the computer where fine resolution is essential in the product, then 10 turn potentiometers can be used. Otherwise we feel that the added speed and simplicity of one-turn multiplying pots makes them preferable. Often the computing loops can be redesigned so that the usually-large signals do not go through multiplying pots. In this way the limited resolution of the one-turn pots will not seriously effect the dynamics of small motions.

When servo-driven pots are used for multiplication, division can be accomplished with the same equipment by using the potentiometer to drive the feedback resistor instead of the input resistor (see Appendix III). At least this method is satisfactory as long as the devisor does not go through zero, a condition which is satisfied where division is required in solving the flight equations.

2.3.5 Function Generation. Closely allied with the problem of multiplication is the problem of generation of nonlinear functions in solving the flight equations. When servo multipliers are used, this is accomplished by making the resistance of the multiplying pot vary nonlinearly as a function of wiper-arm position. Curtiss Wright achieves this by means of special cards for each function; the wire for the potentimeter is wound on the card. The other simulator manufacturers used linear potentiometers which are tapped. By placing the proper padding resistors across adjacent taps the nonlinear characteristic can be approximated by means of straight-line segments. Functions with reverse slopes can be handled by driving one of the intermediate taps at a higher voltage than the end tap.

The Curtiss Wright nonlinear potentiometers have the advantage of allowing smoothly-varying function relationships (providing the slope of the function does not become relatively steep). They have the considerable disadvantage that a replacement pot for each type of function must be available as a spare part. Furthermore, when the tapped-pot method is used, deviation of the straight-line approximation from the smooth curve is usually less than the accuracy of the data from which the smooth curve was obtained. Tapped pots have the advantage of being a standard commercial item, and only a small number of tapped pots need be kept in stock as spares for an entire trainer.

When dc computers are used a number of other methods of function generation are available, including diode-shaping networks, photoformers (cathode-ray

tubes with the function as a mask on the tube face; a photoelectric curve follower closes the loop), and time division methods similar to the time division multipliers (Goldberg, RCA Princeton Labs). Again it is our feeling that none of these systems offers the simplicity, accuracy, and reliability available in the servo-driven tapped pots. As with the servo multipliers we feel that improvements can be made in a dc system by using 400 cycle magnetic amplifiers driving 2-phase motors.

2.3.6 Resolvers. One advantage of ac computer systems is that rectangular to polar and polar to rectangular resolutions can be performed by means of ac resolvers, the rotors of which are positioned directly by servo output shafts. All of the simulator manufacturers employ resolvers of this type. However, one turn sine-cosine nonlinear potentiometers are now available which have the same order of accuracy (better than one percent) as the ac resolvers and which can be used on the output shafts of servos to provide resolution for the dc systems.

2.3.7 Power Supplies. Most of the simulator manufacturers use centralized power supplies for the B voltages for servo and summing amplifiers. However, ERCO and Union Switch and Signal are currently using separate B supplies for single summing and servo amplifiers or for groups of such amplifiers. Although this system somewhat lessens distribution problems with ac computers, its disadvantages of increased power consumption, space, and maintenance far outweigh the advantages. Efficient and highly stable B supplies can be obtained with motor-generators followed by the usual vacuum tube regulation. Temperature-regulated standard cells or VR tubes can be used as reference voltages against which the entire supply can be drift-stabilized.

The ac computers currently used in flight simulators tend to have power and signal distribution problems which make the location of interconnecting cables rather critical. This is because the signals are always ac and hence coupling or pickup between leads, or capacity to ground is always a problem. With a dc system such difficulties are greatly reduced if not eliminated.

CHAPTER 3

IMPROVEMENT OF RELIABILITY AND EASE OF MAINTENANCE AUTOMATIC TESTING CIRCUITS

3.1 Methods for Increasing Reliability

The computer section of flight simulators is a complex electronic device employing hundreds of vacuum tubes. Any system of this type is bound to have reliability problems and require considerable maintenance. Since the reliability of the overall computer is the product of the reliability of the component parts, it becomes clear that a tolerable overall reliability figure requires excellent component reliability. Many reliability analyses have been carried out for electronic systems;* results of such studies indicate that systems employing several hundred or more vacuum tubes must be designed with reliability-conscious engineering.

There are a number of elementary ways to increase reliability. First of all, vacuum tubes are undoubtedly the biggest single cause of failure and should be selected carefully as to tube type and used at conservative ratings (see Section 3.2). Resistor and capacitor components should also be used at conservative power and voltage ratings. Adequate ventilation and cooling is important. In areas of continual high humidity the computer should be located in a dehumidified as well as air-conditioned room. Conservative ratings on cables and connectors are also important. That all of these things contribute to reliability is known throughout the simulator industry, and yet in the desire to cut delivery times and costs many of them have been violated in the present simulators in the field.

A number of the manufacturers and bases agree that the servo power-amplifier tubes (usually 6L6 type) have less life expectancy than many of the other types. The use of magnetic amplifiers for the final power stage in servo amplifiers should greatly increase the reliability of servo multipliers and function generators.

---

* See, for example,[4] "A Study of the Current Status of the Electronic Reliability Problem," R. R. Carhart, Project Rand Research Memorandum 1131, 14 August 1953.

3.2 Importance of Tube Reliability

None of the flight simulators currently in the field or in production employ to any extent special long-life tubes, such as the RCA "Red Tubes," the "Military Control" tubes, etc. It is realized that until recently such tubes have not been on the Armed Forces preferred list because of difficulty of procurement, specifications, etc. However, the life expectancy of these tubes is considerably higher than the regular JAN approved tubes and the slight extra cost in incorporating them in the simulators is more than offset by the increased reliability and decreased tube maintenance requirements.

3.3 Automatic Testing Circuits

One of the extremely difficult maintenance problems in any large computer is the determination of whether or not the computer is solving the equations accurately. It is quite possible for sizable errors to exist in the computer solution without detecting these errors for some time. Even when an error is detected it is often difficult to trace the guilty component. In order to facilitate testing the computer section of flight simulators for satisfactory operation, it is recommended that automatic circuits for this purpose be incorporated in the computer. These can be designed so that a failure in the testing circuit will not make the computer inoperative for normal operation.

For example, initial-condition relays can be incorporated into each of the dc electronic integrators to allow all the integrator outputs to be switched to any desired voltage level (see Appendix IV). In this manner a precisely-selected flight configuration (Mach number, altitude, bank angle, heading, attitude, roll rate, pitch rate, etc.) can be frozen in the computer. The output of every amplifier in the trainer can then be compared with the voltage it should have as a result of this configuration. The comparison can be made automatically by means of a stepping relay, which successively samples the output of each amplifier and compares it with the pre-programmed correct output. Any amplifier outputs which deviate from their correct voltage by more than the maximum allowable value can be detected and automatically recorded. This will immediately tell the maintenance man where the error is and how much it is. A further check will quickly tell whether the trouble results from amplifier malfunction, computing-resistor error, or servo potentiometer error.

To check precisely the dynamic behavior of the computer all the integrators which have to be held with outputs representing the test flight configuration can be released simultaneously and allowed to integrate for some exact preset length of time after which they are again frozen at the output voltages they have at that instant. This can be accomplished by means of hold relays (see Appendix IV). Once again a stepping relay is used to sample successively the output of

each integrator and compare it with the pre-programmed correct output. Any deviations here which did not show up in the first test are most probably the result of integrator errors.

The above tests could be programmed for several representative flight configurations. They would be conducted at least as often as once a day and would almost completely assure correct static and dynamic operation of the trainer. Duration of the tests would be only several minutes. The required telephone-type stepping relays are highly reliable and the overall automatic testing circuit would not add appreciably to the complexity of the computer. For schematic circuit diagrams the reader is referred to Appendix IV.

3.4 Standardization of Computer Sections of Flight Simulators

One of the purposes of the present study program is the investigation of possibilities for standardization of computer sections or portions of computer sections of flight simulators. We have come to the conclusion that it would not be practical to standardize the computer configuration for all types of aircraft because of the wide differences in those aircraft and the equations which represent them. However, from an engineering standpoint it would be completely practical to standardize on computing components such as operational amplifiers and servos, providing a dc system is used. The band-width and zero-stability capabilities of dc amplifiers are so much greater than required for satisfactory trainer operation that little trouble should be experienced in meeting a standard set of specifications. Initial production time, cost, maintenance, and spare-parts requirements should be considerably improved if such a component standardization program can be initiated. The non-engineering problems in implementing such a program may, however, be rather large.

CHAPTER 4

COMPARISON OF AIRCRAFT DYNAMIC PERFORMANCE WITH FLIGHT SIMULATORS

4.1 Importance of Dynamic Simulation

The static performance (steady-state speed, rate of climb, etc.) of flight simulators is naturally of considerable importance and is fairly well covered in the specifications to which the trainers are designed and built. It is also felt that the dynamic performance of simulators is important, even though comparatively few quantitative dynamic requirements are present in the current specifications. Many of the pilot complaints about the simulators at the different bases are directly traceable to poor dynamic performance, particularly with small control-stick motions. Lack of simulator stability, difficulty in holding attitude, small rates of descent, etc., are all symptoms of inadequate resolution of small motions in the computer. However, it is with small motion perturbations that the aircraft is normally flown.

Then too, many of the current aircraft exhibit oscillatory behaviors in both lateral and longitudinal motions. This is the reason for incorporating yaw and pitch dampers in the aircraft. The simulator should also have reasonable facsimilies of these oscillatory motions when the dampers are turned off, particularly for small motions and when the simulator incorporates fire-control systems and is used for practice in intercept attacks.

In this chapter we will compare some dynamic flight test data for the F-86D with dc differential analyzer solutions of the flight equations. This will indicate the amount of correlation which can be expected between simulator and actual aircraft. A few dynamic-response recordings from present simulators in the field will also be presented.

4.2 Comparison of Flight-Test Data with DC Differential Analyzer Results

The flight equations for the F-86D were set up on the dc electronic differential analyzer facility of the Department of Aeronautical Engineering, University of Michigan. In order to assure the most accurate solution of the lateral and longitudinal dynamic motions, solutions which would be completely free of any resolution problems, the equations were linearized about the steady-state flight condition and lateral and longitudinal motions were separated. Aerodynamic coefficients were obtained directly from North American Aviation, Inc.[5] Computer solutions of these equations are compared with flight-test data in Figures 4-1 and 4-2. In Figure 4-1 the lateral transients (dutch-roll motion) are presented for a high altitude and a medium subsonic Mach number. Note that agreement in period of the oscillations and time to damp is fairly good. The flight-test data was obtained by deflecting the rudder and recording the angular rates after release of the rudder.

Agreements of this same order of magnitude (5 to 15% in period and time to damp) were observed for several different altitudes and Mach numbers. **In every case a simulator with a response similar to the computer solution** would certainly be considered an accurate enough dynamic facsimile of the aircraft. The product of inertia I_{xz} was neglected in the equations solved in Figure 4-1. Inclusion of I_{xz} does increase the time to damp appreciably, but the flight-test data agrees better with the equations when $I_{xz} = 0$. This suggests that at least for the F-86D the uncertainty in aerodynamic coefficients causes errors as large as those resulting from failure to include the product of inertia. This statement is undoubtedly not correct for many other current aircraft.

It is also interesting to note that direct solution of the F-86D equations given by ERCO for use in their simulator[6] yields substantial agreement with the curves in Figure 4-1.

In the flight-test data shown in Figure 4-2 the aircraft was released stick-free at about zero degrees attitude after a 2 g pull-up. Period and time-to-damp of the short-period longitudinal (pitching) motion agrees well with the dc computer solution. The curves shown are for a medium-high altitude and a high subsonic Mach number.

More complete curves, a description of the derivation and computer circuits for the linearized equations, and a discussion of changes in dynamic response for various simplifications in the equations are all included in a report on the F-86D currently being prepared.

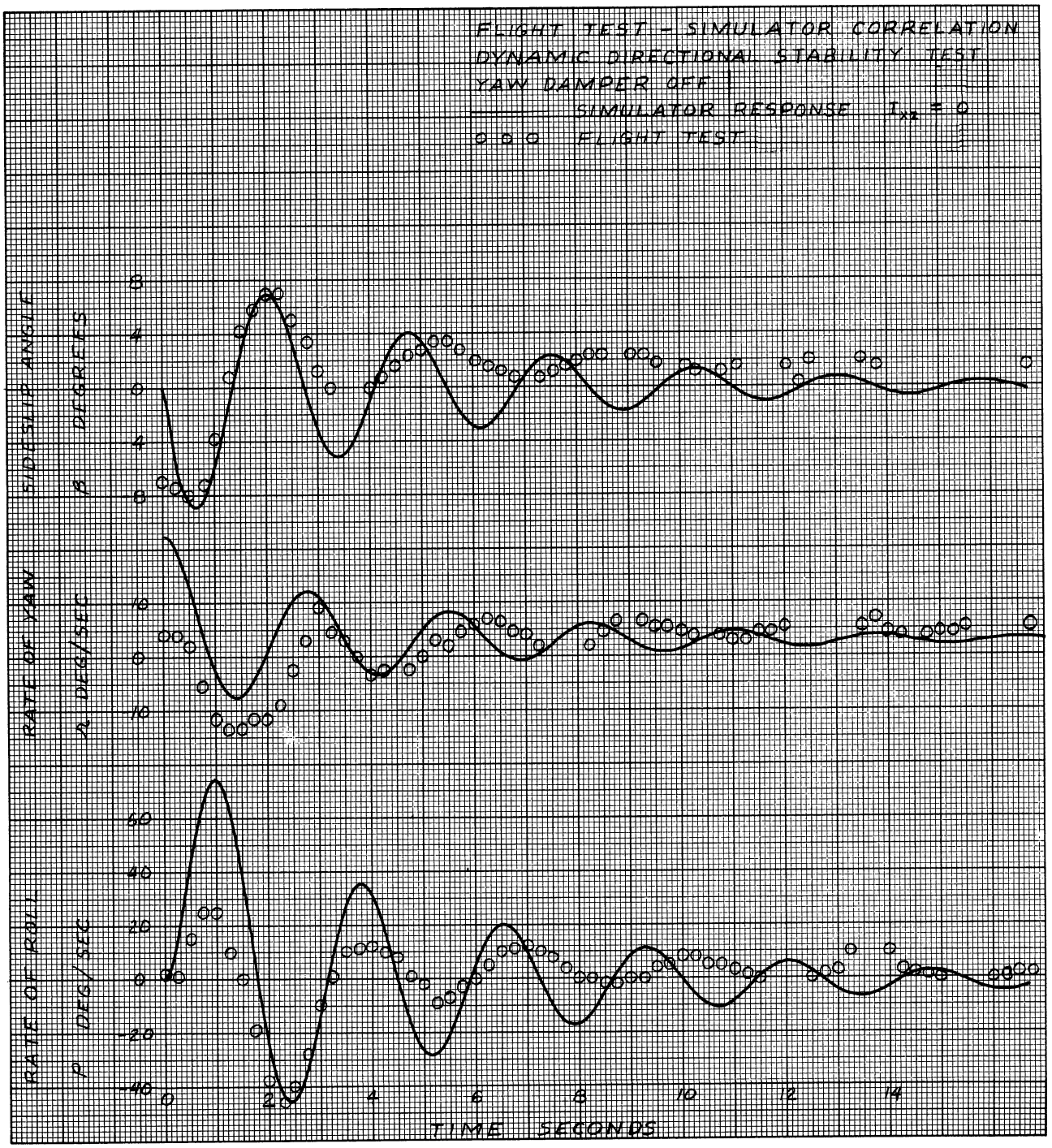

Figure 4-1. Comparison of F-86D Flight-Test Data with Computed Lateral Motions.

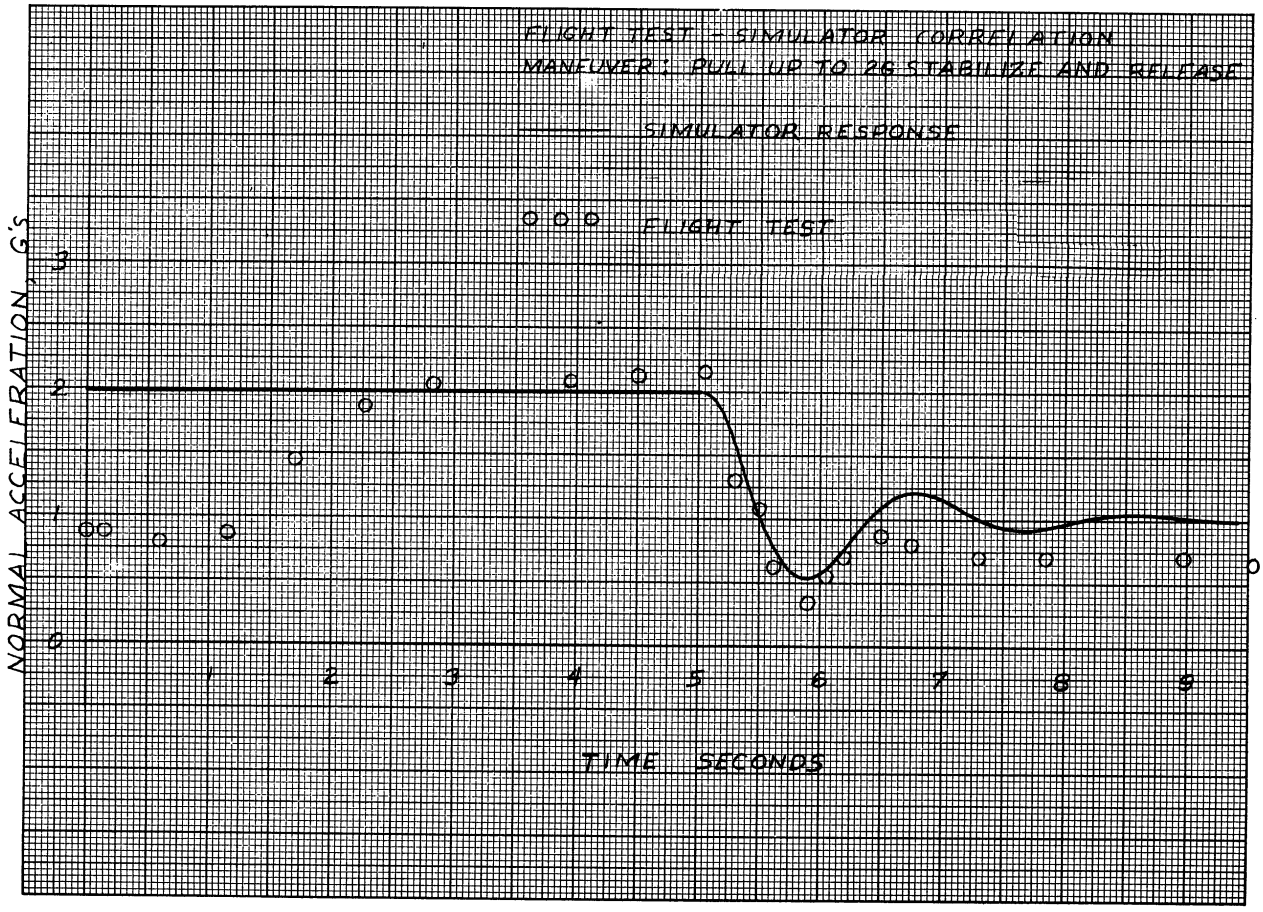

Figure 4-2. Comparison of F-86D Flight-Test Data with Computed Longitudinal Motions.

4.3 Dynamic Performance Tests of Simulators in the Field

In order to observe the dynamic response and small-motion behavior of the ac simulators currently in use, a number of tests were made at three Air Force Bases.

The first tests were run on an ERCO F-86D simulator at Tyndall Air Force Base on January 6, 1954, and January 13, 1954. Recordings of yaw and roll rate were made on a Brush Model BL-202 Oscillograph following rudder displacements of 1.7 and 17 degrees with yaw damper off. No attempt was made to demodulate the 60 cps carrier-modulated output voltages, so that the envelope of the ac recording represents the actual computer roll and yaw rates. In Figure 4-3 several typical runs are shown. As opposed to the flight-test and computed data in Figure 4-1 no dynamic oscillations were observed. The effect of finite resolution capabilities can also be seen in the records as a series of steps instead of smooth curves along the envelope in the recording. The magnitude of these discontinuities is the order of one part in 500 of full scale.

All attempts to trim the simulator in level flight long enough to obtain longitudinal dynamic response data were unsuccessful.

Rudder-kick tests were run on the Curtiss Wright C-124 simulator at West Palm Beach International Airport on January 8 and 9, 1954. Step-function inputs equivalent to rudder-pedal deflections of 1.0 and 10.4 degrees were introduced and yaw and roll rates were recorded from the yaw and roll tachometers respectively. Some typical response data is shown in Figure 4-4. The lateral oscillations (dutch roll) are clearly evident in the curves. Resolution in the output traces was apparently the order of one part in 300 of full scale. We had no C-124 flight-test data with which to compare the lateral dynamics, but the pilots we talked to indicated qualitative agreement between trainer and aircraft. Again the simulator seemed too difficult to stabilize in pitch attitude to obtain good longitudinal-response data.

Tests were run on the Link B-47 trainer at Macdill Air Force Base on January 11, 1954. Simulated rudder-kick tests (with the pilots yaw-damper inoperative) were made, and some of the response data are shown in Figure 4-4. Again we did not have flight-test data for correlation but the dutch-roll oscillations of the trainer seemed similar to those inherent in the aircraft. Resolution appeared to be about one part in 200 to 500 of full scale. In the B-47 trainer we were able to excite both long and short period oscillations in longitudinal motions.

To summarize the tests, they show that the ac computers in the field are in most cases able to simulate the dynamic motions of the aircraft, at least when these motions are large. Small-motion simulation is definitely poor as a

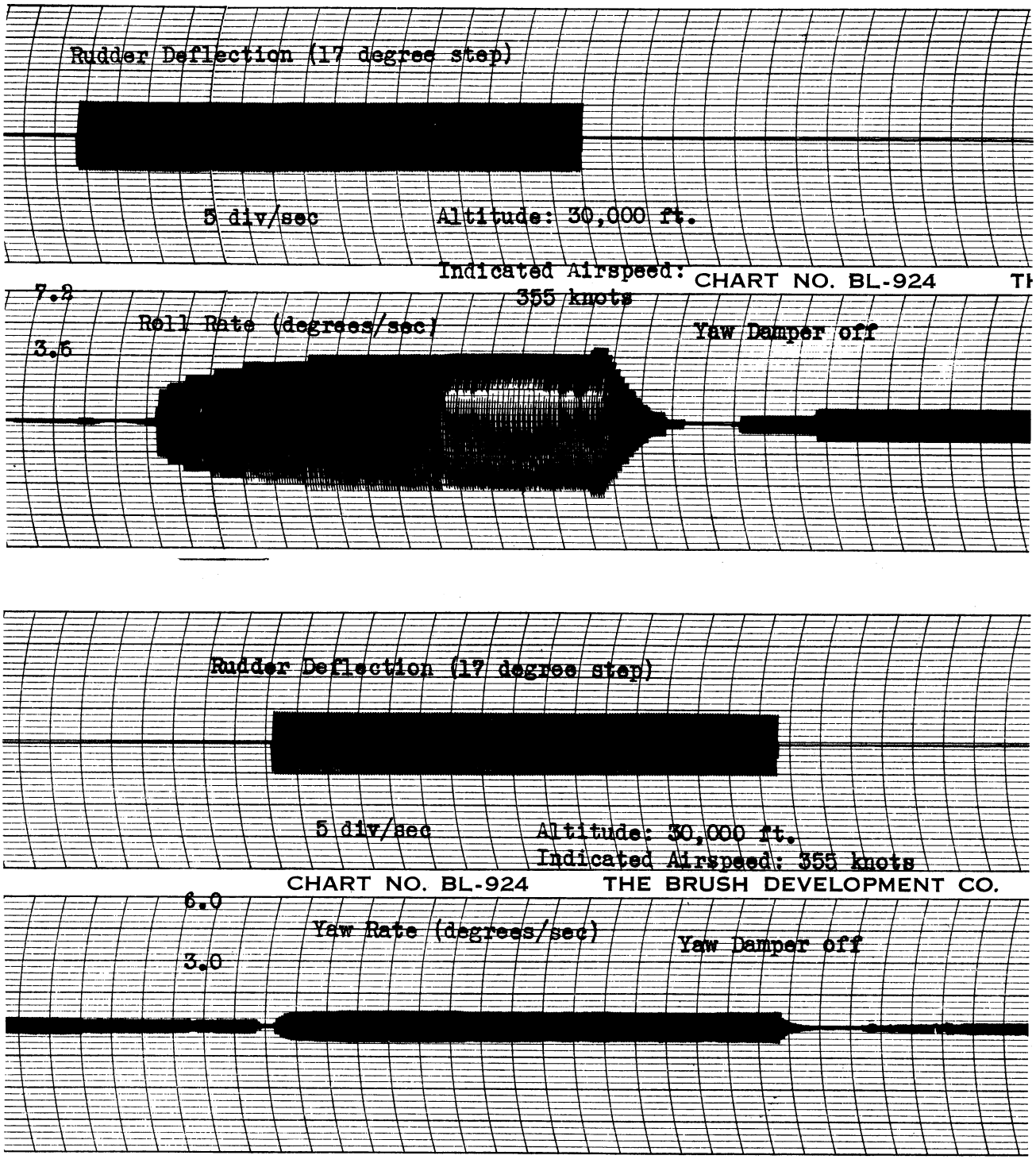

Figure 4-3. Recordings of Lateral Response of ERCO F-86D Simulator.

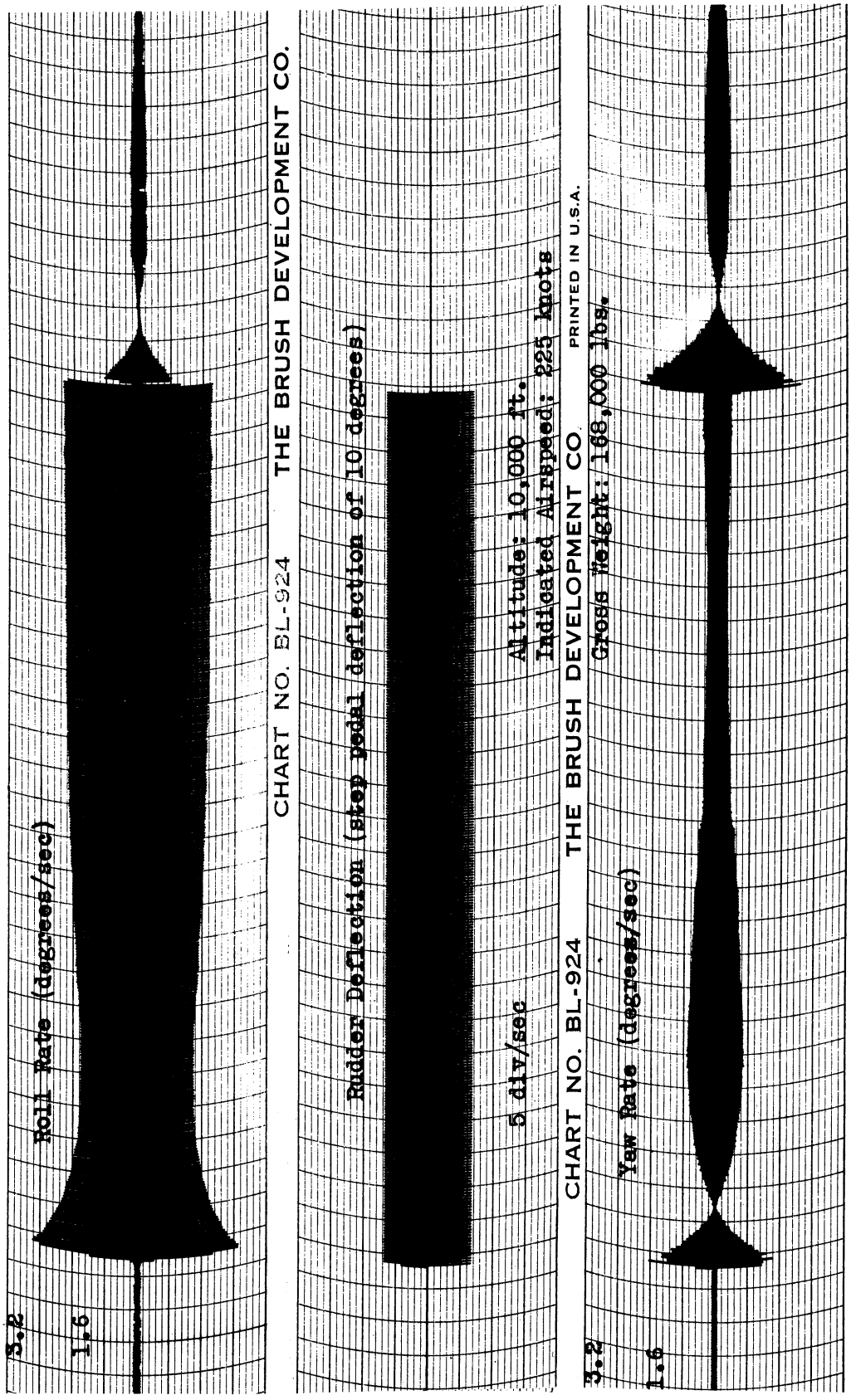

Figure 4-4. Recordings of Lateral Response of Curtiss-Wright C-124 Simulator.

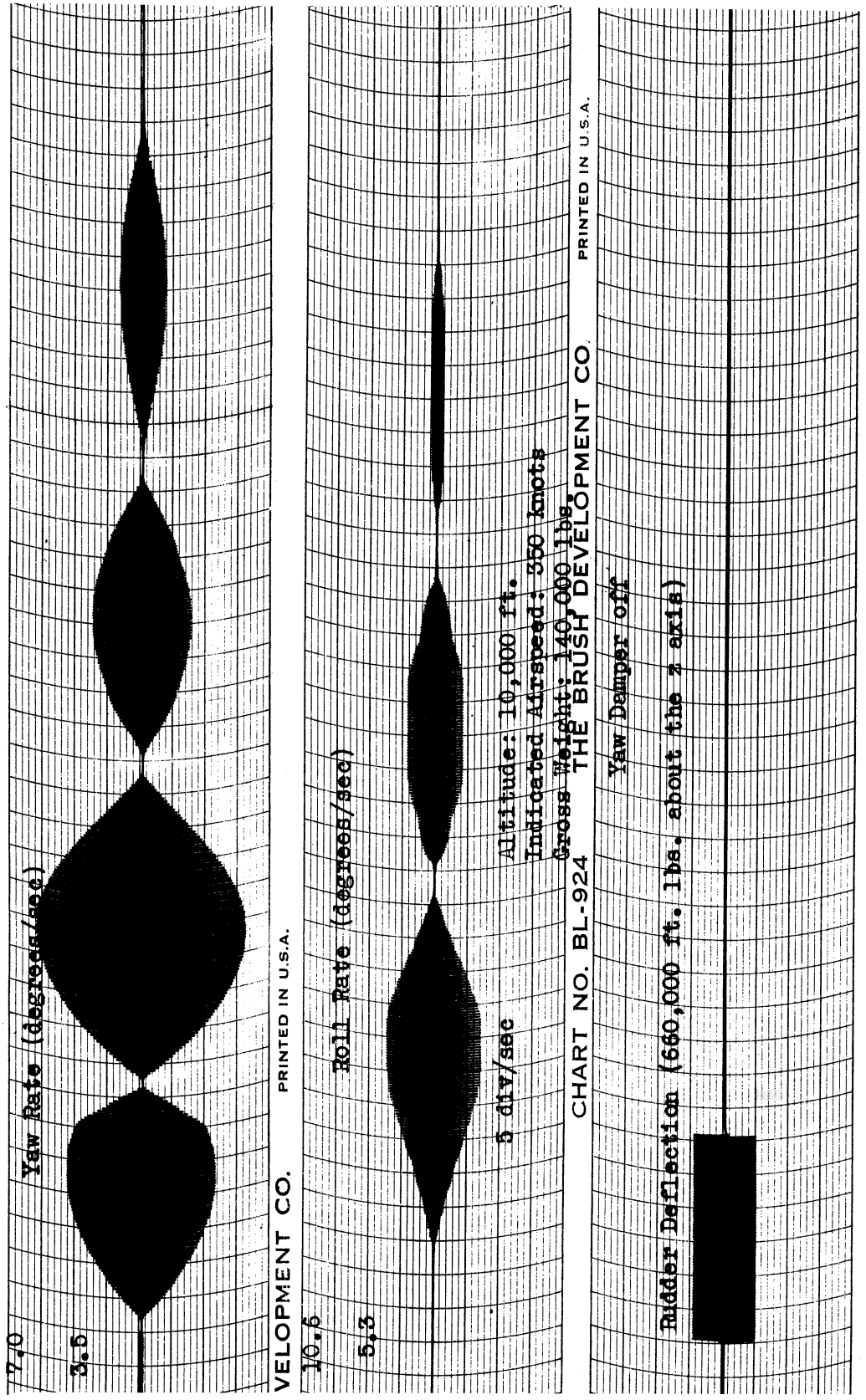

Figure 4-5. Recordings of Lateral Response of Link B-47 Simulator.

result of limited resolution of the ac integrating servos and the followup pots which must be employed. For example, a resolution of one part in 500 in pitch angle (full scale equals ± 90 degrees) corresponds to angle errors of 0.36°. With an airspeed of 300 miles per hour this corresponds to a rate of climb resolution of about 170 feet per minute, which is probably inadequate. At higher forward speeds the equivalent resolution in rate of climb is proportionately worse.

CHAPTER 5

SUMMARY OF SIMULATOR ACTIVITY IN THE AIR FORCE, NAVY, AND AIRCRAFT INDUSTRY

5.1 Simulator Activity in the Air Force

We have already discussed the aircraft training-type flight simulators currently being produced for the Air Force. In addition there are many other companies dealing with Air Force aircraft or missiles which are directly concerned with flight simulators, although more for analysis and design purposes than for pilot training. For example, some of the airframe companies have rather elaborate simulation facilities, and in many cases it is our feeling that developments by these companies are of direct interest in the field of training-type simulators. Although we were able to visit only some of these companies, the results of our visits indicate that much could be gained by more liason between different companies having experience with flight simulators.

North American Aviation, Inc., Inglewood, California, has done considerable simulation work in the design of their fighter-plane control systems. The dc electronic differential analyzers are used to simulate the aerodynamics, and a crude cockpit mockup is included. The stick force simulation felt excellent; it employs a torque-tube drive with feedback to improve greatly the accuracy and smoothness of the forces. Since many of the complaints regarding present training-type simulators have arisen from the stick-force systems, it appears that much could be gained by studying North American and other systems.

Convair, San Diego, has a very elaborate simulation facility employing a dc electronic differential analyzer for solution of the flight equations and a physical cockpit and control-system representation for the rest of the aircraft. Here the stick forces are provided directly by the artificial feel system in the aircraft.

The Hughes Aircraft Company, Culver City, California, has employed a dc flight simulator for a number of years to aid in the design of their fire-control systems. Again the cockpit mockup is crude, and the flight equations

are considerably simplified over those required for the training-type simulators. The Hughes engineers feel that a simple and reliable computer can be built to simulate the airborne fire-control system in trainers for all-weather interceptors. We have already pointed out in our recommendations in Section 1.3 that many of the variables which must be computed in the airborne equipment are available in the flight simulator as voltage outputs and should be utilized directly rather than recomputed. This is, of course, a strong argument against the use of the GFE fire-control equipment in the flight simulators. Since the airborne equipment is also not built for continuous operation over long periods of time, reliability would doubtless be improved by designing a new fire-control computer for the simulation. At least one of the present simulator manufacturers is apparently implementing this philosophy.

Many of the companies involved in guided-missile research have had considerable experience in flight-simulation of missiles. RCA is currently building a very large dc electronic differential analyzer facility for Wright Field which will be used largely for this purpose. Although some of the problems and methods of solution are fundamentally different in such a simulator, the experience of such an organization in solving the flight equations and allied problems should be valuable.

5.2 Simulator Activity in the Navy

The Navy was one of the first to sponsor activity in flight simulation, in the beginning largely for guided missile work. The Cyclone Project at Reeves Instrument Corporation, New York, and the Typhoon Project at RCA, Princeton, are both programs in this field. Both computers are currently using dc electronic differential analyzers although Reeves started with an ac system which was dropped after some time. The computer group at the U.S. Navy Special Devices Center, Sands Point, New York, in addition sponsored a standardized dc computer component development program at Electronic Associates, Inc., Long Beach, New Jersey.

Special Devices Center has also had technical cognizance over the Navy training type flight simulators, which the Navy calls operational flight trainers. In addition to the Air Force simulator manufacturers the Navy is employing Goodyear Aircraft Corporation, Akron, Ohio, as a source of trainers. Although they make dc electronic differential analyzers commercially, Goodyear is using a 400 cps carrier-modulated computing system in their simulators. It is our feeling that the accuracy and resolution difficulties of 60 cps systems will be even more severe with the 400 cps systems.

The Special Devices Center has sponsored for several years a research program at the University of Pennsylvania in the application of digital computers to real-time flight simulation.

We should also mention the simulation facility at the Dynamic Analysis and Control Laboratory of M.I.T. The group here was perhaps the first in the country to turn out useful data in quantity as a result of their missile simulation. They have had considerable experience both with ac and dc computing systems.

The above paragraphs mention the simulator activities which we have visited or with which we are familiar. There are certainly other groups doing active work in the simulation field, and in most cases the results of their labors are available to any group. For example, all of the airframe companies seem willing to talk in detail about their simulation activities. Reluctance of simulator manufacturers themselves to do the same is understandable in view of the fact that producing simulators is their number one business, which it is not in the case of the airframe companies. However, it is our feeling that most of the simulator manufacturers could improve their product by taking more advantage of new computing techniques and simulation developments which are readily available from other companies and research groups.

BIBLIOGRAPHY

1. R. M. Howe, Theory and Operating Instructions for the Air Comp Mod 4 Electronic Differential Analyzer, Report AIR-4, University of Michigan Engineering Research Institute, ONR Contract N6 onr 23223; March, 1953.

2. Korn and Korn, Electronic Analog Computers, McGraw-Hill (1952).

3. Williams, Amey, and McAdam, Wide-Band dc Amplifier Stabilized for Gain and for Zero, Elec. Eng. 68, 934 (1949).

4. R. R. Carhart, "A Study of the Current Status of the Electronic Reliability Problem," Project Rand Research Memorandum 1131, 14 August 1953.

5. North American Aviation, Incorporated, Report NA-50-107A, "Revised F-86D Characteristics for Dynamic Stability and Autopilot Studies."

6. Engineering and Research Corporation, Report No. 6208-20, "Determination of Aerodynamic Equations for the F-86D Flight Simulator."

7. Goodyear Aircraft Corporation, Report GER-4546, "A Survey of Methods of Performing Simulation of the ZPAK Airship in an Operational Flight Trainer," January, 1952.

APPENDIX I

EQUATIONS OF MOTION

I.0 Introduction

The motion of a rigid body in space may be represented by writing six equations of equilibrium corresponding to the body's six degrees of freedom. In this Appendix, the equations of motion are written with respect to a set of axes that are fixed to the airplane.

The forces acting on an airplane in flight are inertia, gravity, thrust, and aerodynamic. Each of these involves special considerations that are treated in the following paragraphs. Translational and rotational inertia forces with respect to a rotating axes system are derived in sections 2 and 3. Gravity forces, being fixed relative to space, require that the orientation of body axes relative to space be defined. This is done in section 4, and the involved relations between orientation rates and angular velocities in the direction of body axes are derived in section 5.

Aerodynamic forces depend upon the orientation of the airplane with respect to the wind, and are most easily developed in a stability axes system. Stability axes are defined in section 7. In section 8, force coefficients are discussed briefly. A detailed discussion of the origin and accuracy of the stability coefficients is given in Appendix II.

Brief statements concerning power forces and control surface inputs are made in sections 9 and 10.

In section 11, all forces are collected and the six equations of equilibrium are written. In the last section, equations are derived from which the position of the aircraft in space may be computed.

I.1 Body Axes

The body axes are an orthogonal right hand set attached to the airplane with the origin of co-ordinates located at the c.g. The x and z axes lie in the plane of symmetry. The x axes is in any convenient fore and aft direction with the positive sense forward. The positive sense for the z direction is towards the bottom of the plane.

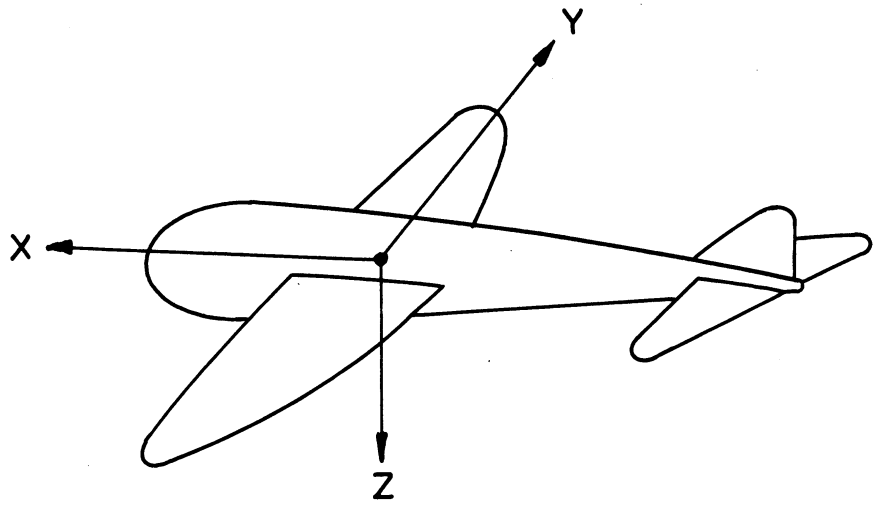

The linear velocity of the airplane $\bar{V}_p$ relative to space is resolved into components U, V, W that have the direction of the body axes.

$$\bar{V}_p = \bar{i}U + \bar{j}V + \bar{k}W$$

From instant to instant any one component, say U, will change its direction relative to space if the airplane is rotating but it will always have the same direction relative to the airplane.

Similarly, the angular velocity of the airplane $\bar{\Omega}$ relative to space is resolved into components P, Q, R in the direction of body axes.

$$\bar{\Omega} = \bar{i}P + \bar{j}Q + \bar{k}R$$

I.2 Translational Inertia Force

The translational inertia force is $-m\,(\delta\,\bar{V}_p/\delta\,t)$ where $(\delta\,\bar{V}_p/\delta t)$ is the time rate of velocity of the airplane as viewed from fixed space. This may be written as the time rate with respect to the rotating body axes plus a time rate due to rotation of the axes relative to space.

$$\bar{V}_p = \bar{i}U + \bar{j}V + \bar{k}W$$

$$\bar{\Omega} = \bar{i}P + \bar{j}Q + \bar{k}R$$

$$\frac{\delta\,V_p}{\delta\,t} = \underbrace{\bar{i}\frac{dU}{dt} + \bar{j}\frac{dV}{dt} + \bar{k}\frac{dW}{dt}}_{A} + \underbrace{U\frac{d\bar{i}}{dt} + V\frac{d\bar{j}}{dt} + W\frac{d\bar{k}}{dt}}_{B}$$

Part A is the time rate of velocity relative to the rotating body axes. Part B is the time rate of velocity due to the rotation of the body axes relative to space. We have:

$$\frac{d\bar{i}}{dt} = \bar{\Omega} \times \bar{i} \qquad \frac{d\bar{j}}{dt} = \bar{\Omega} \times \bar{j} \qquad \frac{d\bar{k}}{dt} = \bar{\Omega} \times \bar{k}$$

Part B becomes

$$\bar{\Omega} \times \bar{i}U + \bar{\Omega} \times \bar{j}V + \Omega \times \bar{k}W = \bar{\Omega} \times \bar{V}_p$$

In vector form:

$$\frac{\delta \bar{V}_p}{\delta t} = \frac{d \bar{V}_p}{d t} + \bar{\Omega} \times \bar{V}_p$$

or in cartesian form, the three components of the translational inertia forces are

$$-m\left\{\dot{U} + WQ - VR\right\}$$

$$-m\left\{\dot{V} + UR - WP\right\}$$

$$-m\left\{W + VP - UQ\right\}$$

I.3 Rotational Inertia Force

By definition, the angular momentum of a body rotating about its c.g. is

$$\bar{H} = \int_{(m)} (\bar{r} \times \bar{q})\, dm$$

where $\bar{r}$ is the distance from the c.g. to dm and $\bar{q}$ is the linear velocity of dm relative to the c.g. If the rotational velocity is $\bar{\Omega}$.

$$\bar{q} = \bar{\Omega} \times \bar{r}$$

and

$$\bar{H} = \int_{(m)} (\bar{r} \times \bar{\Omega} \times \bar{r})\, dm$$

Using the expansion for a triple vector product

$$H = \int_{(m)} \left\{\bar{\Omega}\,(\bar{r} \cdot \bar{r}) - \bar{r}\,(\bar{r} \cdot \bar{\Omega})\right\} dm$$

Letting

$$\bar{\Omega} = \bar{i}P + \bar{j}Q + \bar{k}R$$

$$\bar{r} = \bar{i}x + \bar{j}y + \bar{k}z$$

we get the three cartesian components of $\bar{H}$

$$H_x = \int_m P\,(y^2 + z^2)\,dm - \int_m Q\,xy\,dm - \int_m R\,xz\,dm$$

$$H_y = \int_m Q\,(z^2 + x^2)\,dm - \int_m P\,xy\,dm - \int_m R\,yz\,dm$$

$$H_z = \int_m R\,(x^2 + y^2)\,dm - \int_m P\,xz\,dm - \int_m Q\,yz\,dm$$

The integrals are the moments and products of inertia relative to body axes, and we write finally

$$H_x = PI_{xx} - QI_{xy} - RI_{xz}$$

$$H_y = QI_{yy} - PI_{xy} - RI_{yz}$$

$$H_z = RI_{zz} - PI_{xz} - QI_{yz}$$

The rotational inertia force is $-(\delta\bar{H}/\delta t)$ where $-(\delta\bar{H}/\delta t)$ is the time rate of angular momentum of the airplane as viewed from fixed space. Following the procedure used in getting the translational inertia force, $-(\delta\bar{H}/\delta t)$ becomes

$$-\frac{\delta\bar{H}}{dt} = -\frac{d\bar{H}}{dt} - \bar{\Omega} \times \bar{H}$$

The three cartesian components become

$$-\left\{\frac{dH_x}{dt} + H_z\,Q - H_y\,R\right\}$$

$$-\left\{\frac{dH_y}{dt} + H_x R - H_z P\right\}$$

$$-\left\{\frac{dH_z}{dt} + H_y P - H_x Q\right\}$$

or expanded out

$$-\{\dot{P}I_{xx} - \dot{Q}I_{xy} - \dot{R}I_{xz} + QRI_{zz} - QPI_{xz} - Q^2I_{yz} - RQI_{yy} + RPI_{xy} + R^2I_{yz}\}$$

$$-\{\dot{Q}I_{yy} - \dot{P}I_{xy} - \dot{R}I_{yz} + RPI_{xx} - RQI_{xy} - R^2I_{xz} - PRI_{zz} + P^2I_{xz} + PQI_{yz}\}$$

$$-\{\dot{R}I_{zz} - \dot{P}I_{xz} - QI_{yz} + PQI_{yy} - P^2I_{xy} - PRI_{yz} - QPI_{xx} + Q^2I_{xy} + QRI_{xz}\}$$

arranged in symmetrical form:

$$-\{\dot{P}I_{xx} - (I_{yy} - I_{zz})\,QR - I_{zx}(\dot{R} + PQ) - I_{xy}(\dot{Q} - RP) - I_{yz}(Q^2 - R^2)\}$$

$$-\{\dot{Q}I_{yy} - (I_{zz} - I_{xx})\,RP - I_{zx}(R^2 - P^2) - I_{xy}(\dot{P} + QR) - I_{yz}(\dot{R} - PQ)\}$$

$$-\{\dot{R}I_{zz} - (I_{xx} - I_{yy})\,PQ - I_{zx}(\dot{P} - QR) - I_{xy}(P^2 - Q^2) - I_{yz}(\dot{Q} + RP)\}$$

For airplanes with a plane of symmetry $I_{xy} = I_{yz} = 0$ and we have:

$$-\{\dot{P}I_{xx} - (I_{yy} - I_{zz})\,QR - I_{zx}(\dot{R} + PQ)\}$$

$$-\{QI_{yy} - (I_{zz} - I_{xx})\,RP - I_{zx}(R^2 - P^2)\}$$

$$-\{\dot{R}I_{zz} - (I_{xx} - I_{yy})\,PQ - I_{zx}(\dot{P} - QR)\}$$

I.4 Orientation of Body Axes with Respect to Space

The body axes have zero orientation relative to fixed space when the z axis is in line with gravity and the x axis points due north. Departure of the axes from their zero orientation is measured by the three independent angles ψ, Θ, and Φ. These angles are defined on the following page.

By "vertical plane" is meant any plane that contains the gravity vector. "Horizontal plane" means a plane normal to the gravity vector. xy, yz and zx planes refer to planes containing the body axes. All 5 planes contain the origin of the body axes.

ψ - Heading

Measured in a horizontal plane, and is the angle between due north and the projection of the x axis on the horizontal plane.

Θ - Attitude

Measured in the vertical plane and is the angle between the x axis and the horizontal plane.

Φ - Bank

Measured in the yz plane and is the angle between the y axis and the trace of the yz plane on the horizontal plane.

These angles are independent of each other and completely fix the orientation of the body axes relative to space. The definitions of the angles fail under the following isolated conditions.

ψ fails when Θ is $\pm \pi/2$

Φ fails when Θ is $\pm \pi/2$

The failure of the definitions shows up as infinities in the expressions that use the angles ψ, Θ, and Φ and due account of this must be taken when the equations are mechanized.

ψ, Θ, and Φ are <u>not</u> orthogonal rotations and therefore may not be considered as components of a vector. They have been deliberately named Heading, Attitude, and Bank rather than yaw, pitch, and roll in order to avoid confusion with the components of the angular displacement.

The orientation rates $\dot{\psi}$, $\dot{\Theta}$, $\dot{\Phi}$ are related to the components of the angular velocity P, Q, R in a complicated manner to be derived in the next section.

I.5 $\dot{\psi}$, $\dot{\Theta}$, and $\dot{\Phi}$ in Terms of P, Q, R

In the figure below, zero orientation of the body axes are noted by the subscript (o). Heading, attitude, and bank angles as defined previously are indicated, and the rates $\dot{\psi}$, $\dot{\Theta}$, and $\dot{\Phi}$ occur about the lines with double arrows.

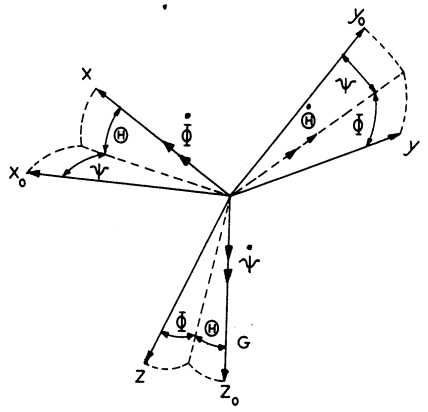

The components of $\dot{\psi}$, $\dot{\Theta}$, and $\dot{\Phi}$ in the directions x, y, z are indicated in the table below.

	x	y	z
$\dot{\psi}$	$-\dot{\psi}\ \text{Sin}\ \Theta$	$\dot{\psi}\ \text{Cos}\ \Theta\ \text{Sin}\ \Phi$	$\dot{\psi}\ \text{Cos}\ \Theta\ \text{Cos}\ \Phi$
$\dot{\Theta}$	-	$\dot{\Theta}\ \text{Cos}\ \Phi$	$-\Theta\ \text{Sin}\ \Phi$
$\dot{\Phi}$	$\dot{\Phi}$	-	-
G	$-\text{G Sin}\ \Theta$	$\text{G Cos}\ \Theta\ \text{Sin}\ \Phi$	$\text{G Cos}\ \Theta\ \text{Cos}\ \Phi$

The sum of the components in the direction of the x axis is P. Q and R are found similarly. We have

$$P = -\dot{\psi}\ \text{Sin}\ \Theta + \dot{\Phi}$$

$$Q = \dot{\psi}\ \text{Cos}\ \Theta\ \text{Sin}\ \Phi + \dot{\Theta}\ \text{Cos}\ \Phi$$

$$R = \dot{\psi}\ \text{Cos}\ \Theta\ \text{Cos}\ \Phi - \dot{\Theta}\ \text{Sin}\ \Phi$$

At any time, the angular velocity components are related to the orientation rates by the above. Inverting, we get (at any time, Θ and Φ are constants and the equations are a linear set in $\dot{\psi}$, $\dot{\Theta}$, and $\dot{\Phi}$).

$$\dot{\psi} = \sec \Theta \, (R \cos \Phi + Q \sin \Phi)$$

$$\dot{\Theta} = Q \cos \Phi - R \sin \Phi$$

$$\dot{\Phi} = P + \tan \Theta \left\{ R \cos \Phi + Q \sin \Phi \right\}$$

Regarding P, Q, and R as knowns, the above is a set of differential equations in Φ, Θ, and ψ.

I.6 Gravity Forces

By definition of zero orientation of the body axes, gravity always acts along Z_o in the diagram above. The components of gravity in the direction of body axes may be taken directly from the table.

$$G_x = - mg \sin \Theta$$

$$G_y = mg \cos \Theta \sin \Phi$$

$$G_z = mg \cos \Theta \cos \Phi$$

The differential equations of the last section may in principle be solved for Φ, Θ, and ψ in terms of P, Q, and R. Therefore, in principle, the gravity components in the direction of body axes may be expressed in terms of P, Q, and R. Actually, it is not possible to find expressions in terms of P, Q, and R explicitly and the problem becomes tractable only if computing machinery is available.

I.7 Orientation of Wind Relative to Airplane - Stability Axes

The stability axes are an orthogonal right hand set with origin located at the airplane c.g. The x_s and z_s stability axes lie in the plane of symmetry. The x_s direction is that of the projection of V_p on the plane of symmetry. The positive sense for x_s and z_s corresponds to that adopted for x and z.

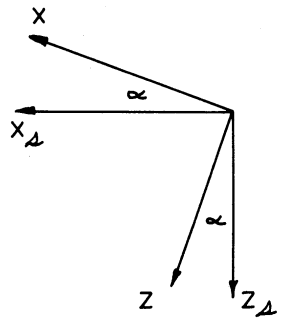

The y axes in the body and stability systems are coincident.

V_p lies in the x_s y_s plane and the angle it makes with the xz body plane is defined as the angle of slip β. Thus

$$U_s = V_p \text{ Cos } \beta$$

$$V_s = V_p \text{ Sin } \beta$$

$$W_s = 0$$

β is positive when the airplane is slipping positively. The component of V_p in the plane of symmetry is located with respect to the body axes by the angle of attack α.

$$\alpha = \tan^{-1} \frac{W}{U}$$

α is positive when W is positive. α and β completely fix the wind relative to the airplane.

I.8 Aerodynamic Forces

Aerodynamic forces arise from the motion of the aircraft (U, V, W, P, Q, R), from an operation of the controls, and from gusts. The forces arising from the motion of the aircraft are given the symbols (X, Y, Z) and the moments are given the symbols (L, M, N).

Forces and moments produced by a displacement of the control surfaces and by gusts are considered to be inputs to the system and are given the symbols (X_c, Y_c, Z_c) and (L_c, M_c, N_c)respectively. It should be noted that if the inputs are forces exerted by the pilot on the controls, then additional equations of motion must be solved in order to find the control surface displacements.

In Appendix II, the forces (X, Y, Z, L, M, N) arising from the motion of the aircraft are discussed in detail. Aerodynamic forces are most conveniently obtained in the stability axes system described in the previous section. Since the y stability and y body axes are coincident, no conversion need be made for the Y force or the moment M about the y axis. Conversion formulae for the other forces and moments may be written directly from the figure below.

$$X = X_s \text{ Cos } \alpha - Z_s \text{ Sin } \alpha$$

$$Z = Z_s \text{ Cos } \alpha + X_s \text{ Sin } \alpha$$

$$L = L_s \text{ Cos } \alpha - N_s \text{ Sin } \alpha$$

$$N = N_s \text{ Cos } \alpha + L_s \text{ Sin } \alpha$$

The forces and moments in the direction of stability axes are given in Appendix II in terms of angular velocities P_S, Q_S, R_S about stability axes and the orientation angles α and β. To complete the conversion, the following formulae connecting the independent variables in the two systems must be used.

$$\alpha = \tan^{-1} \frac{W}{U}$$

$$\beta = \sin^{-1} \frac{V}{V_p}$$

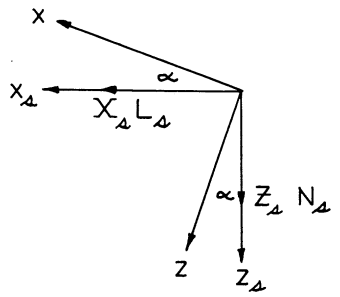

$$P_S = P \cos \alpha + N \sin \alpha$$

$$N_S = N \cos \alpha - P \sin \alpha$$

$$Q_S = Q$$

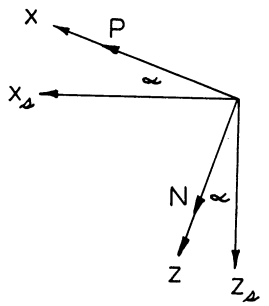

I.9 Power Loads

These are the loads attributable to the operation of the power plant. That is, the difference between the loads on the airplane with power off and power on are called power loads. Various conditions of antisymmetric power can contribute power loads in all six component directions. The three power forces are designated P_X, P_y, and P_Z and the power moments T_X, T_y, and T_Z.

I.10 Control Surface Inputs

Airloads placed on the rigid body by an operation of the controls are given the symbols X_c, Y_c, Z_c, L_c, M_c, N_c. If the inputs are displacements of the control surfaces, the resulting airload inputs are related to the control surface displacements by the airplane geometry. However, if the inputs are forces on the controls, the control surface displacements must be treated as additional degrees of freedom and additional equations of equilibrium must be written.

I.11 Equations of Equilibrium

The six equations of equilibrium in the body axes system are written by summing gravity, inertia, power, aerodynamic and control forces in the 6 component directions.

Translational

$$-mg \sin\Theta - m\{\dot{U} + WQ - VR\} + P_x + X + X_c = 0$$

$$mg \cos\Theta \sin\Phi - m\{\dot{V} + UR - WP\} + P_y + Y + Y_c = 0$$

$$mg \cos\Theta \cos\Phi - m\{\dot{W} + VP - UQ\} + P_z + Z + Z_c = 0$$

Rotational

$$-\{\dot{P}I_{xx} - (I_{yy} - I_{zz})QR - I_{zx}(\dot{R} + PQ)\} + T_x + L + L_c = 0$$

$$-\{\dot{Q}I_{yy} - (I_{zz} - I_{xx})RP - I_{zx}(R^2 - P^2)\} + T_y + M + M_c = 0$$

$$-\{\dot{R}I_{zz} - (I_{xx} - I_{yy})PQ - I_{zx}(\dot{P} - QR)\} + T_z + N + N_c = 0$$

The basic unknowns in these equations are the velocities U, V, W, P, Q, R. ψ, Θ and Φ are related to them through the equations

$$\dot{\psi} = \sec\Theta\,(R\cos\Phi + Q\sin\Phi)$$

$$\dot{\Theta} = Q\cos\Phi - R\sin\Phi$$

$$\dot{\Phi} = P + \tan\Theta\{R\cos\Phi + Q\sin\Phi\}$$

The airforces X, Y, Z, L, M and N depend directly on the velocities. This relationship is derived in a later section. The power forces P_x, P_y, P_z, T_x, T_y, T_z are partly dependent upon the velocities, the remaining part being inputs to the system. The forces X_c, Y_c, Z_c, L_c, M_c, N_c are related directly to the displacement inputs to the control surfaces.

I.12 Position of Aircraft in Space

The orientation of the aircraft in space is given by the angles ψ, Θ, and Φ. When these are known as functions of time it is a simple matter to compute the velocities relative to space.

Body axes in their zero position (see sec. I.5) have the orientation of space axes. From the figure of sec. I.5, it can be seen that velocities in the x_o, y_o, and z_o space directions (due north, due east, and gravity respectively) can be written in terms of U, V, and W as follows.

$$\dot{s}_X = U\,(\text{Cos}\,\Theta\,\text{Cos}\,\psi) + V\,(-\text{Cos}\,\Phi\,\text{Sin}\,\psi + \text{Sin}\,\Phi\,\text{Sin}\,\Theta\,\text{Cos}\,\psi)$$

$$+ W\,(\text{Sin}\,\Phi\,\text{Sin}\,\psi + \text{Cos}\,\Phi\,\text{Sin}\,\Theta\,\text{Cos}\,\psi)$$

$$\dot{s}_y = U\,(\text{Cos}\,\Theta\,\text{Sin}\,\psi) + V\,(\text{Cos}\,\Phi\,\text{Cos}\,\psi + \text{Sin}\,\Phi\,\text{Sin}\,\Theta\,\text{Sin}\,\psi)$$

$$+ W\,(-\text{Sin}\,\Phi\,\text{Cos}\,\psi + \text{Cos}\,\Phi\,\text{Sin}\,\Theta\,\text{Sin}\,\psi)$$

$$\dot{s}_Z = U\,(-\text{Sin}\,\Theta) + V\,(\text{Sin}\,\Phi\,\text{Cos}\,\Theta) + W\,(\text{Cos}\,\Theta\,\text{Cos}\,\Phi)$$

The positions in space s_X, s_y, and s_Z are given by the integrals of $\dot{s}_X$, $\dot{s}_y$ and $\dot{s}_Z$.

APPENDIX II

AERODYNAMICS FORCES

II.0 Introduction

In this Appendix the origin and accuracy of the three translational components of the air force (X, Y, Z) and the three rotational components (L, M, N) are discussed. Air forces are most conveniently obtained in the stability axes system described in section I.7 and all forces, moments, and linear and angular velocities that appear in the present appendix are taken with respect to stability axes. The subscript "s" used previously to distinguish components in the stability axes system will be omitted.

Conversion formulae between body and stability axes are given in section I.8.

II.1 Factors Influencing the Aerodynamic Forces

Except for aeroelasticity problems in which very rapid motions of the structure occur, the influence of acceleration and displacement of the aircraft on the air loads is small and may be neglected. The airloads are taken to depend upon the translational velocity V_p of the airplane, the orientation α and β of the airplane relative to its velocity and the three angular components of the airplane velocity P, Q, and R.

$$X, Y, Z, L, M, N = f_{1,2,\ldots 6}\{V_p, \alpha, \beta, P, Q, R\}$$

In addition to the airplane velocity, the airloads depend upon the properties of the air through which the airplane is flying. Specifically, the viscosity μ, density ρ, and compressibility (characterized by the sonic speed a) of the air enter the problem.

Finally, the geometry of the aircraft as characterized by its shape and size is an important factor. In this connection it should be noted that airplanes are elastic bodies and do not maintain the same shape under all loading conditions. Both the total load and the distribution of the total load may sufficiently distort the structure to change the aerodynamic loading, and this static aeroelastic effect must be taken into account under certain conditions.

II.2 Dimensionless Coefficients

A dimensional analysis will show, that for an airplane of given shape, the aerodynamic forces may be written in non-dimensional form. These so called dimensionless coefficients are defined below.

$$C_X = \frac{X}{\frac{\rho}{2} V_p^2 S} \qquad C_L = \frac{L}{\frac{\rho}{2} V_p^2 S b}$$

$$C_Y = \frac{Y}{\frac{\rho}{2} V_p^2 S} \qquad C_M = \frac{M}{\frac{\rho}{2} V_p^2 S c}$$

$$C_Z = \frac{Z}{\frac{\rho}{2} V_p^2 S} \qquad C = \frac{N}{\frac{\rho}{2} V_p^2 S b}$$

S, b, and c are parameters that characterize the airplane size. S is the wing area, b is the wing span, and c is a characteristic wing chord.

Dimensional analysis shows that each of these coefficients may depend upon the following dimensionless parameters:

α $\qquad$ $\mathrm{Re} = \frac{\rho V_p c}{\mu}$ $\qquad$ Reynolds number

β $\qquad$ $\mathrm{Ma} = \frac{V_p}{a}$ $\qquad$ Mach number

$$\frac{Pb}{2V_p} \qquad \frac{Qc}{2V_p} \qquad \frac{Rb}{2V_p}$$

In addition, due to certain interference effects of the wing and fuselage on the tail, the orientation rates $\dot{\alpha} = d\alpha/dt$ and $\dot{\beta} = d\beta/dt$ may be important. They enter the problem as dimensionless parameters of the form $\dot{\alpha}c/2V_p$ and $\dot{\beta}b/2V_p$.

The results of dimensional analysis are for an airplane of given shape. If the airplane deforms significantly under load, this complicated effect should

be taken into account. A restricted but important special case is one in which the total lift remains constant and equal to the weight. Then the deformation depends upon the load distribution, which in turn depends upon angle of attack. To fly with lift equal to weight at different altitudes but at the same flight speed requires different angles of attack. Therefore, the structural deformation, under lift equal weight conditions can be related to altitude, and the dimensionless coefficients through their dependence on airplane shape become a function of altitude.

II.3 Stability Derivatives

All coefficients except C_X arise primarily from the lifting properties of wing, fuselage, and tail surfaces. Consequently, the influence of Reynolds number on the coefficients other than C_X is small and can usually be neglected. The Mach number, on the other hand, powerfully influences some of the coefficients in the speed range where compressibility effects are important. Altitude, through its influence on elastic distortion also appreciably influences some of the coefficients.

Aerodynamic forces in coefficient form have been used for many years in the study of dynamic stability and response of aircraft. In these analyses, the motion of an aircraft following a small disturbance from equilibrium flight is of interest. Consequently, a good approximation may be had by assuming the coefficients to be linear functions of the velocities. From considerations of symmetry, a linear theory rules out certain couplings among the variables. Specifically, the asymmetric disturbances (β, P, R) cannot cause symmetric forces (X, Z, M) and similarly, the symmetric disturbances (α, $\dot{\alpha}$, Q) cannot produce asymmetric forces (Y, L, N). Consequently, the form of the force coefficients as used in small motion stability analyses is as follows:

$$C_X = \frac{\partial C_X}{\partial \alpha}\,\alpha + \frac{\partial C_X}{\partial\left(\frac{Qc}{2V_p}\right)}\,\frac{Qc}{2V_p} + C_{X_o}$$

$$C_Z = \frac{\partial C_Z}{\partial \alpha}\,\alpha + \frac{\partial C_Z}{\partial\left(\frac{Qc}{2V_p}\right)}\,\frac{Qc}{2V_p} + C_{Z_o}$$

$$C_N = \frac{\partial C_M}{\partial \alpha}\,\alpha + \frac{\partial C_M}{\partial\left(\frac{Qc}{2V_p}\right)}\,\frac{Qc}{2V_p} + C_{M_o} + \frac{\partial C_M}{\partial\,\frac{\dot{\alpha}c}{2V_p}}\,\frac{\dot{\alpha}c}{2V_p}$$

$$C_Y = \frac{\partial C_Y}{\partial \beta}\beta + \frac{\partial C_Y}{\partial\left(\frac{\rho b}{2V_p}\right)}\frac{Pb}{2V_p} + \frac{\partial C_Y}{\partial\left(\frac{Rb}{2V_p}\right)}\frac{Rb}{2V_p}$$

$$C_L = \frac{\partial C_L}{\partial \beta}\beta + \frac{\partial C_L}{\partial\left(\frac{Pb}{2V_p}\right)}\frac{Pb}{2V_p} + \frac{\partial C_L}{\partial\left(\frac{Rb}{2V_p}\right)}\frac{Rb}{2V_p}$$

$$C_N = \frac{\partial C_N}{\partial \beta}\beta + \frac{\partial C_N}{\partial\left(\frac{Pb}{2V_p}\right)}\frac{Pb}{2V_p} + \frac{\partial C_N}{\partial\left(\frac{Rb}{2V_p}\right)}\frac{Rb}{2V_p}$$

The constants of proportionality are the stability derivatives and are given the following symbols:

$$C_{X_\alpha} = \frac{\partial C_X}{\partial \alpha} \qquad C_{Y_\beta} = \frac{\partial C_Y}{\partial \beta} \qquad C_{N_\beta} = \frac{\partial C_N}{\partial \beta}$$

$$C_{X_Q} = \frac{\partial C_X}{\partial Qc/2V_p} \qquad C_{Y_P} = \frac{\partial C_Y}{\partial Pb/2V_p} \qquad C_{N_P} = \frac{\partial C_N}{\partial Pb/2V_p}$$

$$C_{Z_\alpha} = \frac{\partial C_Z}{\partial \alpha} \qquad C_{Y_R} = \frac{\partial C_Y}{\partial Rb/2V_p} \qquad C_{N_R} = \frac{\partial C_N}{\partial Rb/2V_p}$$

$$C_{Z_Q} = \frac{\partial C_Z}{\partial Qc/2V_p} \qquad C_{L_\beta} = \frac{\partial C_L}{\partial \beta} \qquad C_{M_{\dot\alpha}} = \frac{\partial C_M}{\partial \dot\alpha c/2V_p}$$

$$C_{M_\alpha} = \frac{\partial C_M}{\partial \alpha} \qquad C_{L_P} = \frac{\partial C_L}{\partial Pb/2V_p}$$

$$C_{M_Q} = \frac{\partial C_M}{\partial Qc/2V_p} \qquad C_{L_R} = \frac{\partial C_L}{\partial Rb/2V_p}$$

The stability derivatives are constants that depend upon the equilibrium flight condition from which the small disturbance occurs. They depend in general upon the equilibrium values of Ma, Re, α, β, and the airplane shape.

C_{X_o}, C_{Z_o}, and C_{M_o} represent values of the coefficients for the equilibrium value of α. The equilibrium values of β, $Qc/2V_p$, $Pb/2V_p$, and $Rb/2V_p$ are assumed to be zero.

II.4 Adaption to General Motions and Typical Values of the Coefficients

For ordinary motions of an aircraft, the orientation angles α and β and the angular velocities P, Q, and R are generally small enough so that no surface stalls. Therefore, the assumption that the forces vary with α, β, P, Q, and R in the same manner as they do in small disturbance theory has some merit. The stability derivatives, however, are no longer constants, for they themselves must be expressed as functions of α, β, Ma and altitude, where elastic distortion is important.

There is little doubt that the forces are non-linear functions of the velocities and orientation when any but small disturbance problems are considered. By allowing the stability derivatives to be variable, some of these non linearities are introduced. Whether or not this procedure takes care of all the important non-linearities is conjectural, but it represents the state of the art at the present time.

The aerodynamics force coefficients for large motions using the variable stability derivative concept are written

$$C_X = C_{X_\alpha}\,\alpha + C_{X_Q}\,\bar{Q} + C_{X_o}$$

$$C_Y = C_{Y_\beta}\,\beta + C_{Y_P}\,\bar{P} + C_{Y_R}\,\bar{R}$$

$$C_Z = C_{Z_\alpha}\,\alpha + C_{Z_Q}\,\bar{Q} + C_{Z_o}$$

$$C_L = C_{L_\beta}\,\beta + C_{L_P}\,\bar{P} + C_{L_R}\,\bar{R}$$

$$C_M = C_{M_\alpha}\,\alpha + C_{M_Q}\,\bar{Q} + C_{M_o} + C_{M_{\dot\alpha}}\,\dot{\bar{\alpha}}$$

$$C_N = C_{N_\beta}\,\beta + C_{N_P}\,\bar{P} + C_{N_R}\,\bar{R}$$

C_{X_o}, C_{Z_o} and C_{M_o} represent the values of the corresponding coefficients when α is zero. $\bar{P}$, $\bar{Q}$, $\bar{R}$, and $\dot{\bar{\alpha}}$ are non dimensional angular velocities.

$$\bar{P} = \frac{Pb}{2V_p} \qquad \bar{Q} = \frac{Qc}{2V_p}$$

$$\bar{R} = \frac{Rb}{2V_p} \qquad \bar{\dot{\alpha}} = \frac{\dot{\alpha}c}{2V_p}$$

The values of the derivatives vary widely with the type of aircraft, angle of attack, and Mach number and altitude of operation. In order to give some idea of the orders of magnitude involves, a typical set of values that might apply to a high speed fighter type aircraft is shown in the table below. The aircraft is operating at a lift coefficient of 0.5 and is flying at Mach 0.7 at 40,000 feet.

C_{X_α}	= - .35	C_{L_β}	= - .06
C_{X_Q}	= 0	C_{L_P}	= - .7
C_{X_o}	= - .02	C_{L_R}	= + .1
C_{Y_β}	= - .4	C_{M_α}	= - .48
C_{Y_P}	= + .005	C_{M_Q}	= -8.0
C_{Y_R}	= + .09	$C_{M_{\dot{\alpha}}}$	= + .5
C_{Z_α}	= -6.0	C_{M_o}	= + .01
C_{Z_Q}	= -2.2	C_{N_β}	= + .08
C_{Z_o}	= - .1	C_{N_P}	= - .015
		C_{N_R}	= - .04

II.5 Origin and Estimated Accuracy of the Coefficients

The stability derivatives, or various combinations of them may be deduced with varying degrees of accuracy from steady state and transient flight test data. From a design standpoint, it is important to estimate the derivatives before a full scale airplane is completed. This is generally accomplished by using flight test data from similar airplanes, by conducting wind tunnel tests on a scale model of the airplane in question, and by calculation from the aerodynamic theory of wings and bodies. Frequently, all three devices must be

used in combination to predict the value of a particular derivative. In general, it can be said that prediction methods that rely heavily on pure theory are least accurate.

In this section each of the stability derivatives is discussed briefly from the standpoint of how they arise and what parameters such angle of attack, Mach number, Reynolds number, and structural distortion may be expected to influence them. Finally, an attempt has been made to assess the probable accuracy with which each may be predicted.

II.5.1 Lift - C_{Z_α}

C_{Z_α} is the negative of the lift curve slope of the airplane as a whole and is negligibly influenced by Reynolds number below the stall. The effects of Mach number and elastic distortion of the wing are pronounced at high speeds. Theory indicates that the lift curve slope for a rigid wing increases with Mach number until the transonic range is reached. Theoretical results at transonic speeds are unreliable. Elastic twisting and bending of the wing can change the sectional angles of attack and thereby influence the lift curve slope. If the lift is maintained equal to the weight, changes in center of pressure relative to the elastic axis will result in a variable twisting moment. This is a source of variation of lift curve slope with altitude.

The lift curve slope can be deduced from flight test data with good accuracy, probably within 5%. Wind tunnel tests usually involve rigid models and correction for distortion must be made theoretically. A completely theoretical estimate of lift curve slope of the elastic airplane probably cannot be made with greater accuracy than 15%.

II.5.2 Drag - C_{X_o}, C_{X_α}

C_{X_o} is the negative of the drag coefficient at zero lift. It arises from the form and skin friction drag of the airplane and can be expected to decrease slightly with increasing Reynolds number. The effect of structural deformation is probably small. The variation with Mach number (at constant Reynolds number) is small until the divergence Mach number is reached. At this point C_{X_o} rises rapidly and may reach several times its sub-divergence value in the transonic range. The theory of wings and bodies does not provide a reliable method of predicting C_{X_o}. Flight or wind tunnel tests can probably provide a value of C_{X_o} within 10%.

C_{X_α}, the drag due to lift, arises from the change in effective angle of attack produced by the spanwise flow around the wing tips. Since C_X due to

lift varies roughly as the square of the lift coefficient, C_{X_α} is proportional to $\alpha C_{Z_\alpha}^2$ and therefore shows a dependence on Mach number and elastic distortion. The effect of Reynolds number below the stall is small. C_{X_α} can be predicted from theory or estimated from wind tunnel or flight test data. Accuracy from theoretical predictions is probably not greater than 15%; from flight or wind tunnel test, probably not greater than 10%.

II.5.3 Side Force Derivative - C_{Y_β}

Side force due to side slip arises primarily from the vertical tail acting as a lifting surface. However, because of powerful interference effects from the horizontal tail, wing, and fuselage, theoretical predictions are not accurate. Force tests on a model at an angle of yaw to the wind tunnel stream must be made. Contributions of the wing, fuselage, and wing-fuselage interference on the tail vary sufficiently with lift coefficient so that C_{Y_β} should be measured over a range of angles of attack.

C_{Y_β} will vary with Mach number because both interference effects and the vertical tail lift curve slope vary with Mach number. This coefficient is very likely a function of β for large angles of slip. It probably can be measured in the wind tunnel to within 10%.

II.5.4 Static Stability Derivatives C_{M_α}, C_{L_β}, C_{N_β}

The static stability derivatives are a measure of the restoring moments generated by a displacement α_1, and β_1 from the orientation at which all aerodynamic moments about the c.g. vanish in non-maneuvering flight. They are readily measured in the wind tunnel by placing the model at various angles of attack and yaw with respect to the wind stream. Fair estimates can be made from aerodynamic theory of the contribution of some of the airplane components to the derivatives. However, powerful interference effects make theoretical estimates for the airplane as a whole unreliable. C_{M_α} can be measured indirectly in flight, but flight testing for C_{L_β} and C_{N_β} is impractical.

C_{M_α} receives major contributions from the wing and tail through the lift variation with angle of attack of these surfaces. The contribution of the fuselage is generally small. Downwash at the tail from the wing is an important effect. Propeller and jet power plants both contribute to this derivative in a manner that cannot be reliably predicted by theory. Since C_{M_α} depends upon the lift curve slopes of wing and tail, it is strongly influenced by Mach number and structural deformation. It can probably be predicted from wind tunnel tests to within 15%.

The effective dihedral C_{L_β} arises from the geometric dihedral and sweep of the wings, from interference effects between wings and fuselage, from the sweep and dihedral of the horizontal tail, and from the displacement of the center of pressure of the vertical tail from the roll axis. The asymmetric distribution of the slip stream over the wings during a slip is also an important factor at low speeds. C_{L_β} is sensitive to angle of attack and Mach number and can probably be predicted from wind tunnel tests to within 20%.

The largest contributions to the directional stability C_{N_β} comes from the vertical tail. Due account must be taken of sidewash interference effects from the fuselage on the tail. The fuselage itself contributes a large increment to the derivative that cannot be predicted theoretically. The contribution of straight wings is small but becomes appreciable for large angles of sweep. Both propeller and jet power plants contribute to C_{N_β}. The part of C_{N_β} that cannot be reliably predicted theoretically is a large part of the whole and therefore wind tunnel data should be used. C_{N_β} will depend upon angle of attack and Mach number. For some configurations, structural distortion is important. Estimates from wind tunnel tests can probably be made to within 20%.

II.5.5 Damping Derivatives C_{L_P}, C_{M_Q}, C_{N_R}

Direct measurements of the damping derivatives in flight are not feasible, though some of them can be deduced if reliable information on control power is available. In the wind tunnel, C_{L_P} can be measured with a rolling balance or it can be deduced from oscillation tests. Oscillation tests in pitch and yaw will yield the combinations $C_{M_Q} + C_{M_{\dot\alpha}}$ and $C_{N_R} + C_{N_{\dot\beta}}$. $C_{M_{\dot\alpha}}$ and $C_{N_{\dot\beta}}$ must be estimated in order to extract the desired damping derivatives. Whirling arms have also been used to measure C_{M_Q} and C_{N_R}. In general, the direct contributions of the lifting surfaces to the damping derivatives are large compared to interference effects and fair estimates of C_{M_Q} and C_{L_P} can be made from theory.

The damping in roll C_{L_P} results predominantly from the wings. It increases with aspect ratio and decreases with taper and sweep. In most cases, the fuselage contribution is negligible. The horizontal tail acts qualitatively like the wings but its contribution is small. At high angles of attack the side force due to rolling on the vertical tail can have a sufficient moment arm about the roll axis to make a significant contribution. C_{L_P} depends upon angle of attack and Mach number. In some configurations, distortion may be important. Damping in roll can probably be estimated to within 15%.

Damping in pitch C_{M_Q} is contributed mostly by the horizontal tail, though the effects of fuselage and wing cannot be neglected. Because of the time lag between the generation of wing downwash and its action on the horizontal tail, a damping moment is produced that is proportional to $\dot\alpha$. This is usually computed

theoretically and subtracted from the damping moment measured in the wind tunnel. The important parameter involved in C_{M_Q} is the lift curve slope of the horizontal tail, which in turn depends upon Mach number and structural distortion. Damping in pitch can probably be predicted within 20%.

Like the damping in pitch, the damping in yaw C_{N_R} comes from the angle of attack generated on the vertical tail by the yawing velocity. The fuselage is relatively more important in the yaw case and its contribution depends upon the fuselage cross section and angle of attack. The lift curve slope of the vertical tail which depends upon Mach number is the important parameter. Damping in yaw can probably be predicted within 30%.

II.5.6 Cross Derivatives C_{N_P} and C_{L_R}

Like the damping derivatives, the cross derivatives are not directly measureable in flight. They can be deduced from wind tunnel tests, though the required instrumentation is not generally available. The cross derivatives are usually estimated from theory and as a result, the accuracy is poor.

The yawing moment due to rolling velocity C_{N_P} is contributed for the most part by the wing and vertical tail. The tilt of the lift vector during a positive roll produces a negative yawing moment that is proportional to the lift coefficient. A rolling velocity generates an angle of attack distribution on the vertical tail that produces a positive or negative yawing moment depending upon the location of the vertical tail relative to the roll axis. The sidewash on the vertical tail from the rotation of the wings is difficult to estimate theoretically and leads to inaccuracy in the prediction of the derivative. C_{N_P} is a function of angle of attack, Mach number, and distortion. A theoretical estimate can probably be made within 50%.

The rolling moment due to yawing velocity C_{L_R} is also caused predominately by the wing and vertical tail. The differential lift on the wings generated by a positive yawing velocity produces a positive rolling moment proportional to the lift coefficient. A positive yawing velocity also produces an angle of attack on the vertical tail that results in a rolling moment. Interference effects of the wing-body on the vertical tail must be taken into account. C_{L_R} is a function of angle of attack, Mach number and distortion. A theoretical estimate can probably be made within 50%.

II.5.7 Force-Rotary Derivatives C_{X_Q}, C_{Z_Q}, C_{Y_P}, C_{Y_R}

The forces arising from rotational velocities cannot be directly obtained in a practical manner from either wind tunnel or flight test. They

are obtained either by purely theoretical means or by deducing their values from measurements on the damping derivatives. The accuracy with which they may be predicted is poor. Fortunately, these derivatives are small quantities and are generally unimportant.

An angular velocity of pitch generates an angle of attack on the horizontal tail thereby increasing both the lift and drag of the tail. This is the primary source of the derivatives C_{X_Q} and C_{Z_Q}. C_{X_Q} is always small and need not be considered. C_{Z_Q} is roughly equal to the damping in pitch, C_{M_Q}, divided by the non dimensionalized tail length. It is influenced by Mach number to the extent that the interference effects on the horizontal tail and the tail lift curve slope are influenced by Mach number. It can probably be estimated to within 30%.

A velocity of yaw R generates an angle of attack on the vertical tail in the same manner that a velocity of pitch Q generates an angle of attack on the horizontal tail. C_{Y_R} is roughly equal to the part of the damping in yaw C_{N_R} contributed by the vertical tail divided by the non dimensionalized tail length. C_{Y_R} is a function of angle of attack and Mach number. On some configurations the wing contributes to a side force due to yawing velocity. C_{Y_R} can probably be predicted from C_{N_R} to within 30%.

The side force due to rolling C_{Y_P} is a small quantity that arises from the wing and vertical tail. It depends upon angle of attack and Mach number and can probably be estimated from C_{N_P} to within 50%.

APPENDIX III

THEORY OF ELECTRONIC DIFFERENTIAL ANALYZERS

III.0 Introduction

As a result of this study program we are recommending the use of a dc electronic differential analyzer type of computer to replace the ac computers currently used in the flight simulators. In order to orient the reader who may not be completely familiar with the theory of operation of dc electronic differential analyzers we have included this Appendix with the report.

III.1 DC Operational Amplifiers

The basic unit of the dc electronic differential analyzer is the operational amplifier, shown schematically in Figure III-1a. It consists of a dc amplifier having a gain $-\mu$, an input impedance Z_i, and a feedback impedance Z_f. The input voltage to the dc amplifier proper is e' and its output voltage is e_2. If we neglect any current into the dc amplifier (it can usually be made less than 10^{-10} amps), then the currents through input and feedback impedances must be equal. Thus by Ohms law

$$\frac{e_1 - e'}{Z_i} = \frac{e' - e_2}{Z_f} \qquad \text{(III-1)}$$

where e_1 is the input voltage to the operational amplifier. But by definition $e' = -e_2/e_1$, so that we can solve Equation (III-1) for e_2, obtaining

$$e_2 = \frac{-\frac{Z_f}{Z_i}}{1 + \frac{1}{\mu}\left(1 + \frac{Z_f}{Z_i}\right)} e_1 \qquad \text{(III-2)}$$

For the amplifier gain $\mu \gg Z_f/Z_i$, Equation (III-2) reduces to

$$e_2 = -\frac{Z_f}{Z_i} e_1 \qquad \text{(III-3)}$$

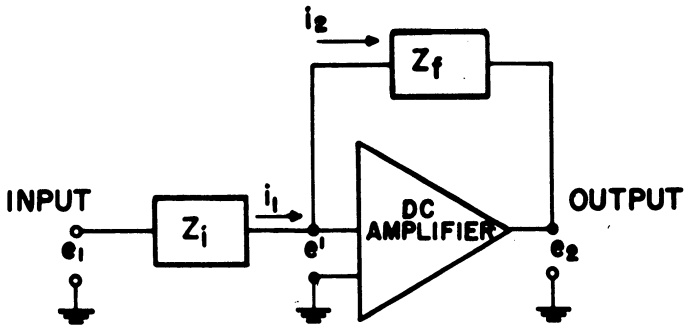

$$e_2 = -\frac{Z_f}{Z_i} e_1$$

a.) OPERATIONAL AMPLIFIER

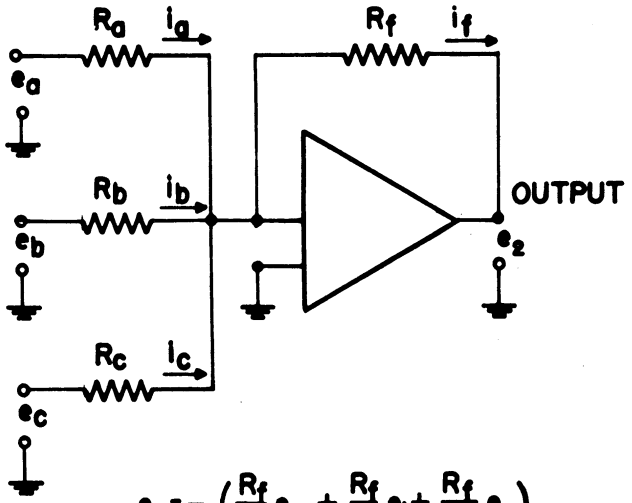

$$e_2 = -\left(\frac{R_f}{R_a} e_a + \frac{R_f}{R_b} e_b + \frac{R_f}{R_c} e_c\right)$$

b.) OPERATIONAL AMPLIFIER AS A SUMMER

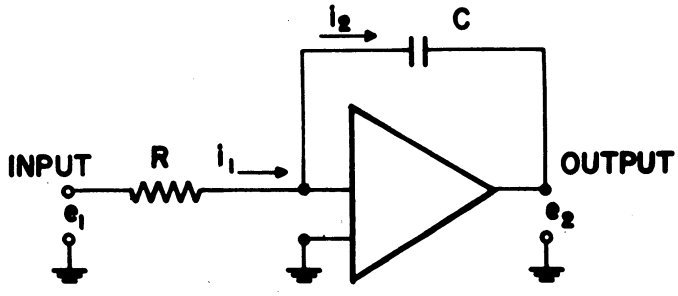

$$e_2 = -\frac{1}{RC} \int e_1 \, dt$$

C.) OPERATIONAL AMPLIFIER AS AN INTEGRATOR

Figure III-1. Operational Amplifiers

which is the fundamental equation governing the behavior of the operational amplifier. For Z_i and Z_f resistors, we can multiply any voltage e_1 by a constant K by making the ratio of feedback to input resistance equal to K. The output voltage e_2 will be $-Ke_1$, as required, except for a sign reversal.

By employing several input resistors R_a, R_b, and R_c with a single feedback resistor R_f, the operational amplifier can be used to sum input voltages e_a, e_b, and e_c. Thus in Figure III-1b currents $i_a + i_b + i_c = i_f$, and by Ohms law

$$\frac{e_a - e'}{R_a} + \frac{e_b - e'}{R_b} + \frac{e_c - e'}{R_c} = \frac{e' - e_2}{R_f} \qquad \text{(III-4)}$$

If we neglect e' as small compared with e_a, e_b, e_c or e_o ($e' = -e_2/\mu$ where μ is very large), then Equation (III-4) can be solved for e_2. Thus

$$e_2 = -\frac{R_f}{R_a} e_a - \frac{R_f}{R_b} e_b - \frac{R_f}{R_c} e_c \qquad \text{(III-5)}$$

The output voltage e_2 is the sum of the three input voltages e_a, e_b, and e_c, each multiplied respectively by the ratio of feedback to input resistance. Hence, the operational amplifier can be used to multiply by constants and sum voltages.

Finally, consider the operational amplifier shown in Figure III-1c. Here the input impedance is a resistor R and the feedback a capacitor C. Again neglecting any current into the amplifier proper and assuming that e' is negligibly small compared with e_1 or e_2, we have

$$i = \frac{e_1}{R} \text{ and } -e_2 = \frac{1}{C}\int i\, dt$$

from which

$$e_2 = -\frac{1}{RC}\int e_1\, dt \qquad \text{(III-6)}$$

Thus the output voltage is proportional to the time integral of the input voltage. The constant of proportionality is 1/RC, and RC is known as the time constant of the integrator.

We have seen how dc operational amplifiers can be used for multiplication by a constant, sign reversal, summation, and integration. The basic operating principles of servo multipliers, dividers, and function generators are

described in Section III.3. Let us now turn to more detailed design and performance considerations for dc operational amplifiers.

III.1.1 Stability Considerations

Since the operational amplifier is essentially a feedback device, it is important to design the attenuation-frequency characteristic of the dc amplifier so that it will be stable when the feedback and input impedances are added. From Equation (III-2) the output voltage e_2 is given by

$$e_2 = -\frac{Z_f}{Z_i}\,\frac{\mu(p)}{\mu(p) + \left(1 + \frac{Z_f}{Z_i}\right)}\,e_1 \qquad \text{(III-7)}$$

where the dc amplifier gain $\mu(p)$ actually includes time-derivative terms, as indicated by the fact that it is a function of the differential operator p. If the operational amplifier is to be stable, the denominator of Equation (III-7) must not vanish for any values of p with positive real part. This is apparent when we realize that the roots of the denominator are the characteristic roots of the equation of motion of the operational amplifier.

When resistors R_f and R_i are used for feedback and input impedances respectively, the roots of the denominator of Equation (III-7) are the values of p for which $\mu(p) = -(1 + R_f/R_i)$. If none of these p values is to have positive real parts, the phase shift of the amplifier gain $\mu(j\omega)$ for sinusoidal inputs ($p = j\omega$) must not be as negative as 180 degrees at the frequency where the magnitude of $\mu(j\omega) = 1 + R_f/R_i$. This in turn implies that a db gain versus log frequency plot of $\mu(j\omega)$ for sinusoidal inputs must not have a slope as negative as -12 db per frequency octave in the region where $|\mu(j\omega)| = 1 + R_f/R_i$. For a conservative design, a slope of -6 dc/octave is preferred. (This corresponds to about -90 degrees phase shift). If the operational amplifier is to be stable for all possible ratios R_f/R_i, then the db gain versus log frequency characteristic of the dc amplifier proper should have a slope of -6 db/octave down to below unity (zero db) gain. The frequency response of a typical dc amplifier is shown in Figure III-2. For an operational gain of 5 or less (one would usually try to design the computer circuit so that this is true) the dc amplifier with the characteristic shown in Figure III-2 would have a frequency response flat to 5000 cps or higher.

Normally there is an upper frequency limit beyond which the gain of dc amplifiers falls off very rapidly (e.g., at -6 db/octave for each triode stage

due to grid to plate capacity). Stabilization is often obtained by purposely reducing the gain of one of the amplifier stages. This can be done by connecting a capacitor from grid to plate to cut down the overall amplifier gain at - 6 db/octave, starting at a low enough frequency so that the gain is down to unity before the gain of the other stages begins to fall off with frequency.

When the dc amplifier is used as an integrator (feedback capacitor C, input resistor R), the ratio $Z_f/Z_i = 1/j\,\omega\,RC$ for sinusoidal inputs. At the frequency ω where $|\,\mu(j\omega)\,| = 1 + Z_f/Z_i$ the term Z_f/Z_i is negligible compared with 1, and the stability consideration is virtually the same as for zero feedback resistance in the previous case. Thus the amplifier attenuation characteristic shown in Figure III-2 insures that the operational amplifier will be stable for integration as well as for summation and multiplication by a constant.

III.1.2 Drift Analysis

Next let us consider the problem of zero drift in the dc operational amplifiers. A dc amplifier must be balanced so that with zero input voltage the output voltage is zero. This balance can, in a properly designed dc amplifier, usually be achieved by slight changes in the operating conditions of the first stage of vacuum-tube amplification. Once the amplifier has been balanced, subsequent changes in heater voltage, B voltages, ambient temperature, etc., may cause the amplifier to drift off of balance so that zero voltage input no longer gives zero voltage output.

In Figure III-1a assume the operational amplifier has an input resistor R_i and a feedback resistor R_f. If we consider the effect of amplifier unbalance, the output voltage e_2 is given by

$$e_2 = -\mu\,(e' + e_B)\,, \qquad \text{(III-8)}$$

where $-\mu$ is the amplifier gain, e' is the dc amplifier input voltage, and e_B is the voltage unbalance of the dc amplifier referred to its input. Equating input and feedback currents we have

$$\frac{e_1 - e'}{R_i} = \frac{e' - e_2}{R_f}\,, \qquad \text{(III-9)}$$

where e_1 is the input voltage to the operational amplifier. Eliminating e' in Equation (15) by means of Equation (14) we have

$$e_2\left[1 + \frac{1}{\mu}\left(1 + \frac{R_f}{R_i}\right)\right] = -\frac{R_f}{R_i}\,e_1 - \left(1 + \frac{R_f}{R_i}\right)e_B \qquad \text{(III-10)}$$

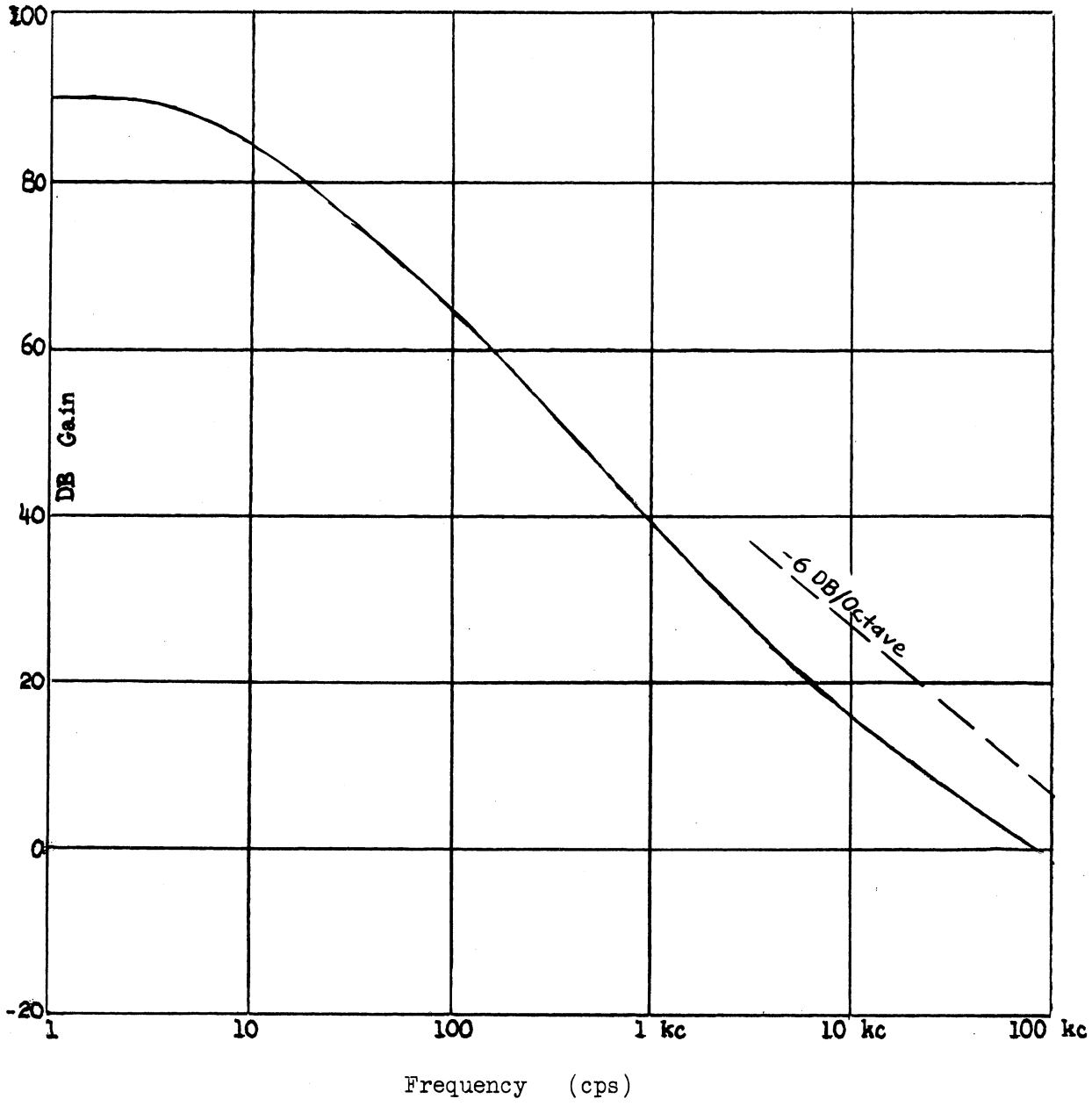

Figure III-2. Typical Open-Loop Frequency Response of a DC Amplifier.

For $\mu \gg R_f/R_i$

$$e_2 = -\frac{R_f}{R_i} e_1 - \left(1 + \frac{R_f}{R_i}\right) e_B \qquad \text{(III-11)}$$

and the unbalance at the output (i.e., the output voltage when $e_1 = 0$) is given by

$$e_2\,(0) = -\left(1 + \frac{R_f}{R_i}\right) e_B, \quad \mu \gg R_f/R_i \qquad \text{(III-12)}$$

where we recall that e_B is the voltage unbalance referred to the input. Thus the larger the ratio R_f/R_i (i.e., the larger the gain of the operational amplifier), the larger the voltage drift or unbalance at the output.

The voltage unbalance e_B referred to input may be quite small compared with the voltage change which caused e_B. For example, if e_B resulted from a 1 volt shift in plate voltage of the first stage of triode amplification, and if the gain of the first stage were 30, then e_B would be 1/30 volt. i.e., a 1/30 volt change in input voltage e' would produce an equivalent unbalance.

In dc amplifiers employing a 5691 twin triode input stage[1] with a common cathode bias resistor, we have observed that the average expected drift e_B referred to input is the order of 5 to 15 millivolts over a period of a number of days. Filament and B supplies for the amplifiers were, of course, well regulated. Warmup time required for e_B to settle down within 15 millivolts of the steady-state value is the order of 10 to 30 minutes. A 10 millivolt unbalance referred to input will, according to Equation (III-12), give a 20 millivolt offset at the amplifier output when the amplifier is used at unity gain ($R_f = R_i$). If full scale is 100 volts this represents an amplifier unbalance of one part in 5000 of full scale. For this reason we feel, in the simulator application, that drift of dc operational amplifiers will, in general, offer no problems.

III.1.3 Drift Stabilized dc Operational Amplifiers

In the previous section we saw that with well-regulated power supplies the expected zero-drift of manually balanced dc operational amplifiers over periods of days would be the order of 20 millivolts for unit-gain summers. With integrators involved in closed-loop computations (the pilot essentially closes the loop with regard to attitude and position in flying the simulator) this unbalance appears quite unimportant. However, the integrators which compute north and east coordinates from the velocity components in those directions must be

considered more carefully, since here the computation is essentially an open-ended one. For this reason we are including here a discussion of drift-stabilized dc amplifiers.

The drift-stabilized dc amplifier includes the addition of a drift-free amplifier, as shown in Figure III-2a. The additional ac amplifier may consist of a synchronous vibrator or chopper which converts the dc input voltage e' to an ac signal (usually 60 cycles) the magnitude of which is proportional to e'. This ac signal is sent through an ac amplifier and reconverted to dc by means of another pair of contacts on the same synchronous vibrator. The net result is a drift-free dc amplifier, the output of which is supplied to an additional input e'' to the main dc amplifier. The way in which this drift-free amplifier improves the performance of the operational amplifier is described below.

Assume that the unbalance in the main dc amplifier in Figure III-3 is e_B volts referred to input. Then the output e_o is given by

$$e_o = -\mu (e' + e'' + e_B) \qquad \text{(III-13)}$$

where e' and e'' are equally effective inputs to the amplifier, and where μ is the main dc amplifier gain. Let the gain of the drift-free amplifier be G, and assume that this amplifier has an offset equal to e_C volts when referred to input. (This offset may result from chopper contact voltage or stray pickup in the ac amplifier at the chopper frequency.) Then the output e'' of the drift-free amplifier is

$$e'' = G (e' + e_C) \qquad \text{(III-14)}$$

If we neglect any current flow into the main dc amplifier or the auxiliary, drift-free amplifier, then Equation (1) gives us the relationship between the input voltage e_1 to the operational amplifier and the output voltage e_o. Combining Equations (1), (8), and (9), we have

$$e_o = \frac{1}{1 + \frac{1}{\mu(1+G)}\left(1 + \frac{Z_f}{Z_i}\right)} \left[-\frac{Z_f}{Z_i} e_1 - \left(1 + \frac{Z_f}{Z_i}\right)\left(\frac{e_B}{1+G} + \frac{G}{1+G} e_C\right)\right] \qquad \text{(III-15)}$$

The effective gain of the amplifier before feedback has evidently been increased from μ to $\mu (1 + G)$. Since the auxiliary drift-free amplifier cannot pass frequencies higher than one half the vibrator frequency (60/2 = 30 cps for a 60 cps chopper), it is necessary to use low-pass filters on both input and output sides of this amplifier. Thus the gain of the drift-free amplifier may be considerable at dc and very low frequencies, but falls off rapidly at higher frequencies. At high frequencies the effective gain of the overall amplifier before feedback is μ, while at low frequencies it is $\mu (1 + G)$.

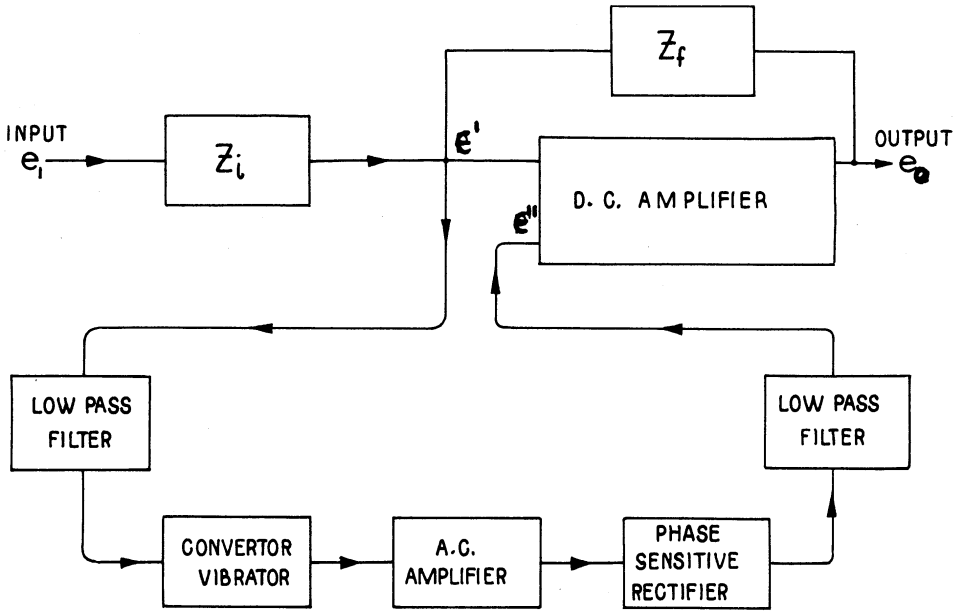

Figure III-2a. Drift-Stabilized Amplifier.

Consider Equation (10) when the operational amplifier input e_1 equals zero. If $\mu\ (1 + G) \gg 1 + Z_f/Z_i$ and if $G \gg 1$, then

$$e_o\ (0) \cong -\left(1 + \frac{Z_f}{Z_i}\right)\left(\frac{e_B}{1 + G} + e_C\right) \qquad \text{(III-15)}$$

This equation represents the voltage unbalance in the output resulting from voltage unbalance e_B in the main dc amplifier and unbalance e_C in the drift-free amplifier. Clearly the introduction of the auxiliary chopper amplifier has reduced the unbalance e_B in the main dc amplifier by a factor $1 + G$, where G is the gain of the chopper amplifier. It is also evident that there is no reason for having G larger than required to make $e_B/(1 + G) < e_C$, since no matter how large G is made, we are still left with an unbalance of $(1 + Z_f/Z_i)e_C$. In practice e_C can be held to 10^{-4} volts or less, whereas e_B depends upon the regulation of the power supply voltages and the constancy of the environmental conditions. Typical values for μ are 10^4 to 10^5 and for G, 400-2000.[1,2,3] The total unbalance referred to input can be made less than 100 μ volts.

III.1.4 Design Considerations

It is felt that the dc operational amplifiers for the computer section of simulators should have three stages of amplification. A twin triode with a single cathode resistor seems best for the first stage (e.g., 5691 or 6SU7), followed perhaps by two stages of triode amplification in a single twin-triode envelope. A cathode follower tube or tubes can be used following the final amplification stage. Not only will this make the frequency response of the amplifier (and hence its stability) virtually independent of any capacitance on the output load but it also allows a single amplifier circuit and layout to be used for several different output power requirements. By providing a socket at the amplifier output for the cathode follower tube the amplifier can be used with or without cathode follower output merely by plugging in the proper tube into the output socket. A toggle switch can be thrown to convert the amplifier output lead from the plate of the last amplifier tube to the cathode of the cathode-follower tube. For example, amplifiers which are used to drive high impedances such as summing resistors could be used without cathode-follower output, whereas those used to drive servo potentiometers would use cathode-follower output. In this way a considerable power saving would be made in the computer section.

Another possible combination of tubes for the dc amplifier would be a twin triode input stage as suggested above, followed by a pentode and finally a twin triode. The first section of the final low-power twin triode would provide the last stage of amplification. The second stage, a cathode follower, would be used at all times as an output stage. An additional high-power cathode-follower could be plugged in when needed as described in the previous paragraph.

Power supplies needed for the dc amplifiers include well-regulated B+ and B- supplies (e.g., +300 and -350 volts) for the plate and output bias voltages on the three amplification stages. In addition, less regulated but higher-power B+ and B- supplies (e.g., ± 190 volts) should be used for the plate and cathode-resistor voltages of the cathode follower output stages (the B- voltage is also used on the cathode of the last amplification stage). The first two well-regulated supplies need only supply several milliamps per amplifier, while the latter two supplies might require several tens of milliamps per high-power amplifier.

For non drift-stabilized amplifiers ac filament voltage should be satisfactory. A dc filament voltage may be necessary for amplifiers with drift-stabilization if such amplifiers are required.

III.2 Static and Dynamic Errors in DC Summing and Integrating Amplifiers

In deciding on the performance requirements of dc amplifiers for solution of the flight equations it is important to understand the static and dynamic errors of summing and integrating amplifiers resulting from their non-ideal behavior.

III.2.1 Zero Drift Errors of Summers

We have already discussed in Section III.1.2 the output unbalance of a dc amplifier as a result of unbalance e_B referred to input. In the case of a summing amplifier employing several input resistors R_a, R_b, R_c, ... and a feedback resistor R_f it is easy to show that the output unbalance e_2 (0) is given by

$$e_2\,(0) \cong -\left(1 + \frac{R_f}{R_a} + \frac{R_f}{R_b} + \frac{R_f}{R_c} + \ldots.\right) e_B \qquad \text{(III-16)}$$

From this Equation one can compute the expected drift in the output of a summer. If, for example, the drift $e_B \cong 10^{-2}$ volt over a one-week period for an unstabilized dc amplifier, then the resulting output drift for a summer with R_a = 1 meg, R_b = 0.5 meg, R_c = 0.5 meg and R_f = 1 meg is equal to 10^{-2} (1 + 1 + 2 + 2) = 6×10^{-2} or 60 millivolts.

III.2.2 Dynamic Errors of Summers

In Section III.1.1 we saw that a conservative open-loop frequency-response characteristic for a dc amplifier exhibited a slope of -6 db per octave down to zero db gain. If we let ω_o equal the frequency at which the amplifier

gain equals unity ($\omega_o \cong 80$ kc in Figure III-2), then the open-loop transfer function $\mu(p)$ of the dc amplifier is given by

$$\mu(p) = \frac{\mu_o}{\tau p + 1}, \quad \tau = \frac{\mu_o}{\omega_o} \tag{III-17}$$

where μ_o is the dc gain of the amplifier and τ is a time constant equal approximately to the frequency at which the gain begins to fall off from μ_o. From Equations (III-2) and (III-17) the output voltage e_o of an operational summer with feedback resistor R_f and input resistor R_i is given by

$$e_o = -\frac{R_f}{R_i} \frac{1}{1 + \left(\frac{1}{\omega_o} p + \frac{1}{\mu_o}\right)\left(1 + \frac{R_f}{R_i}\right)} e_1$$

or

$$e_o \cong -\frac{R_f}{R_i} \frac{1}{\frac{1}{\omega_o}\left(1 + \frac{R_f}{R_i}\right)p + 1} e_1 \tag{III-18}$$

$$\mu_o \gg 1 + \frac{R_f}{R_i}$$

Thus the amplifier has a steady-state gain or static sensitivity equal to $-R_f/R_i$, but has an effective time lag $(1/\omega_o)(1 + R_f/R_i)$. For a step input voltage e_1 this means that the amplifier response e_o will approach $-(R_f/R_i)e_1$ exponentially, rising to 1/2.72 of the final value in $(1/\omega_o)(1 + R_f/R_i)$ seconds. From Equation (III-18) the frequency response of the summer can readily be computed. In practice the amplifier gain usually falls off at somewhat lower frequencies than predicted by Equation (III-18), depending on the impedance of the summing resistors.

III.2.3 Drift of Integrators

Next, let us examine the output drift of integrators because of amplifier unbalance or due to grid current. If the latter exists, then in Figure III-1c the total current i_2 through the feedback capacitor is given by $i_1 + i_g$, where i_g is the grid current. Thus the voltage across C is

$$e' - e_2 = \frac{1}{C}\int i_2\, dt = \frac{1}{C}\int \left(\frac{e_1 - e'}{R} + i_g\right) dt$$

Eliminating e' from Equation III-8 and denoting $\int dt$ by p^{-1} we have for the output voltage e_2 of the integrator

$$e_2 = -\frac{1}{1+\frac{1}{\mu}\left(1+\frac{1}{RCp}\right)}\left[\frac{1}{RCp}e_1 + \left(1+\frac{1}{RCp}\right)e_B + \frac{i_g}{Cp}\right] \qquad \text{(III-19)}$$

or if $\mu \gg 1/RCp$

$$e_2 \cong -\left[\frac{1}{RCp}e_1 + \left(1+\frac{1}{RCp}\right)e_B + \frac{i_g}{Cp}\right] \qquad \text{(III-20)}$$

We should, of course, add a constant e_2 (0) to Equation (III-20) as a result of the initial charge on the feedback condenser C. The effect of a constant unbalance e_B referred to the dc amplifier input is now clear; due to the $(1/RCp)e_B$ term in Equation (III-20) it causes an additional output voltage $(e_B/RC)t$ to build up linearly as a function of time. For example, if R = two megohms, C = one microfarad (RC = two seconds), and $e_B = 10^{-2}$ volts, the integrator output voltage builds up at a rate of one volt per 200 seconds in addition to the desired output

$$-\frac{1}{RC}\int e_1\,dt\ .$$

Thus the effect of the amplifier unbalance is to cause an integrator output drift equivalent to an input signal e_B.

The effect of grid current i_g is also clear from Equation (III-20); it, too, causes the integrator output to increase linearly as a function of time. For example, if $i_g = 10^{-9}$ amps and C = one microfarad, the integrator output builds up at a rate of one volt per 1000 seconds. Note that the grid current effect is independent of the input resistor R and depends only on the integrating capacitor C. Note also that what we have called i_g may result either from electron or ion current to the grid of the input stage of amplification, or may result from leakage current to the grid external to the tube.

III.2.4 Dynamic Errors of Integrators

Now that we have considered integrator drift effects due to amplifier unbalance and grid current, it is important to consider dynamic errors of integration, both for very high and very low frequency inputs. For the open-loop amplifier transfer function μ (p) given in Equation (III-17) we can solve for the dynamic integrator output voltage e_2, obtaining from Equation (III-19) when $e_B = i_g = 0$.

$$e_2 = -\frac{1}{RCp}\left[\frac{1}{1+\left(\frac{1}{\omega_o}p+\frac{1}{\mu_o}\right)\left(1+\frac{1}{RCp}\right)}\right]e_1 \qquad \text{(III-21)}$$

For sinusoidal inputs e_1 having high frequencies ($\omega \gg 1/RC$, $p = j\omega$)

$$e_2 \cong -\frac{1}{RCp}\left[\frac{1}{\frac{1}{\omega_o}p+1}\right]e_1 \qquad \text{(III-22)}$$

Evidently the integrator output exhibits a time lag of $1/\omega_o$ seconds, where ω_o is the frequency at which the open-loop dc amplifier gain equals unity.

For sinusoidal inputs having very low frequencies ($\omega \ll 1/\omega_o$)

$$e_2 \cong -\frac{\mu_o}{\mu_o RCp + 1} \qquad \text{(III-23)}$$

where μ_o is the dc gain of the amplifier. Thus the integrator actually acts as a summer with gain μ_o and a time constant of μ_o RC seconds. This is also equivalent to an ideal integrator with a leakage resistance of μ_o R in parallel with the feedback capacitor. As a result the amplifier will generate considerable errors if asked to perform open-ended integrations over time periods of the order of μ_o RC seconds. For integrators used to compute north and east coordinates, RC can be made very large so that the above effect, along with the effect of amplifier unbalance, would probably be small enough to make manually-balanced dc amplifiers acceptable. However, the effect of grid current discussed in the previous section can cause important errors unless the feedback capacitor C is large enough. For $i_g = 10^{-10}$ amps and C = 10 microfarads (both reasonable figures) the integrator drift from grid current i_g would be one volt per 100,000 seconds or about 0.03 volts per hour, undoubtedly an acceptable figure.

III.3 Servo Multipliers and Function Generators

Thus far we have discussed the use of dc operational amplifiers for the linear operations of multiplication by a constant, sign inversion, summation, and integration. Let us now review briefly the principles of operation of servo multipliers and function generators.

III.3.1 Servo Multiplier

In Figure III-3 the block diagram of a servo multiplier is shown. It consists of a number of linear potentiometers ganged together and driven by a servo motor. The reference voltage $\pm V_R$ is connected across one of the pots, and the voltage αV_R at the potentiometer wiper arm is subtracted from the voltage Z. The resulting error signal $\epsilon = Z - \alpha V_R$ is sent through a high-gain servo amplifier and applied to the servo motor. The motor drives the arm of the pot in the proper direction to reduce the error to zero, i.e., to make $\alpha V_R = Z$. In this way the wiper-arm position on all of the ganged pots is proportional to the voltage Z. If $\pm X$ and $\pm Y$ are applied across each of the remaining two pots in Figure III-3, it is apparent that the wiper-arm voltages will be XZ/V_R and YZ/V_R respectively. Thus the servo multiplier can generate output voltages proportional to the product of input voltages.

Normally the response of the servo amplifier in Figure III-3 must be somewhat higher in the region of the closed-loop natural frequency of the servo. This "error-rate" damping can be accomplished by using the operational amplifier circuit shown in Figure III-4, where a regular dc computing amplifier is used to sum and amplify the voltages Z and $-\alpha V_R$, increase the high-frequency components and drive a magnetic amplifier. The output of the magnetic amplifier in turn drives the variable-phase winding of a two-phase ac servo motor.

III.3.2 Use of Servos for Division

In solving for the aerodynamic forces and moments in the flight equations it is necessary to perform the operation of division. This can be accomplished by using the potentiometer of a servo multiplier in the feedback loop of an operational amplifier, as shown in Figure III-5. If the voltage Z is used to position the wiper arm of the potentiometer, the amplifier output voltage is equal to $(X/Z)V_R$, where-X is the amplifier input voltage and V_R is the reference voltage. This circuit will operate satisfactorily as long as the divisor Z does not go to zero (this condition is met in the computer requirements for flight simulators). One should also note that the feedback resistor R acts as a load resistor on the pot and should be large compared with the pot resistance to prevent appreciable potentiometer loading errors. This error can, of course, be eliminated in any case by loading the servo reference pot with the same resistance R.

The above comments on potentiometer loading effects apply equally well when the pot is used for multiplication; the input resistor of the amplifier following the multiplier pot acts as a load to ground on the wiper arm and must be relatively large or compensated for.

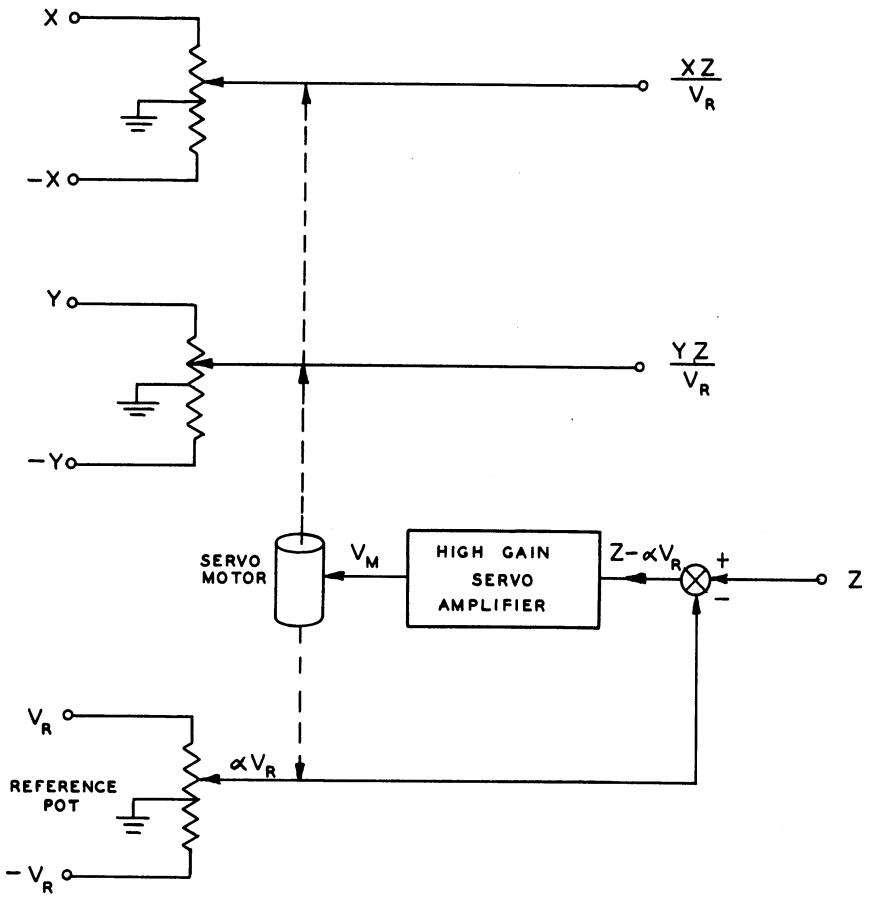

Figure III-3. Servo Multiplier.

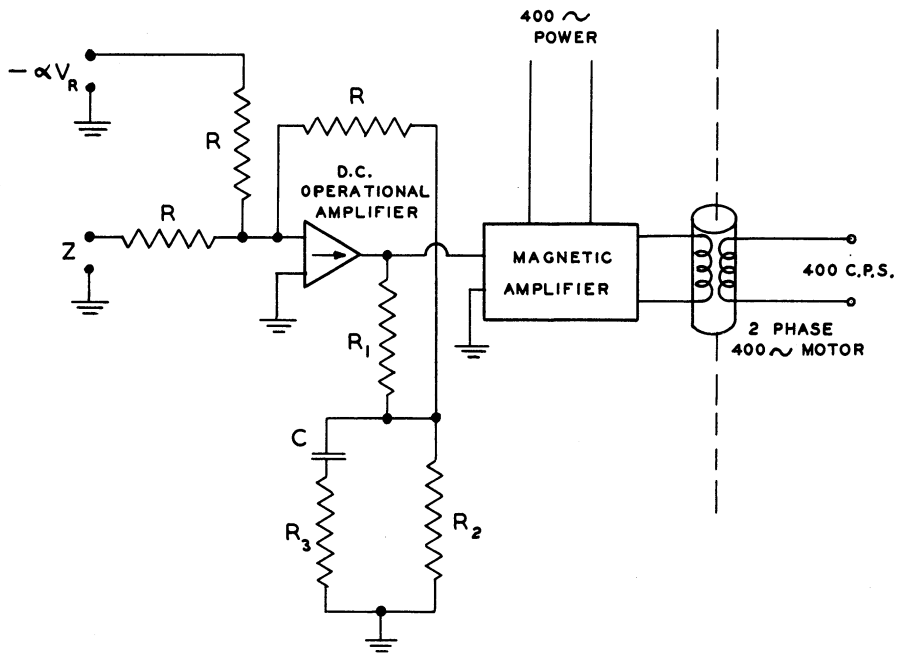

Figure III-4. Schematic of Servo Amplifier.

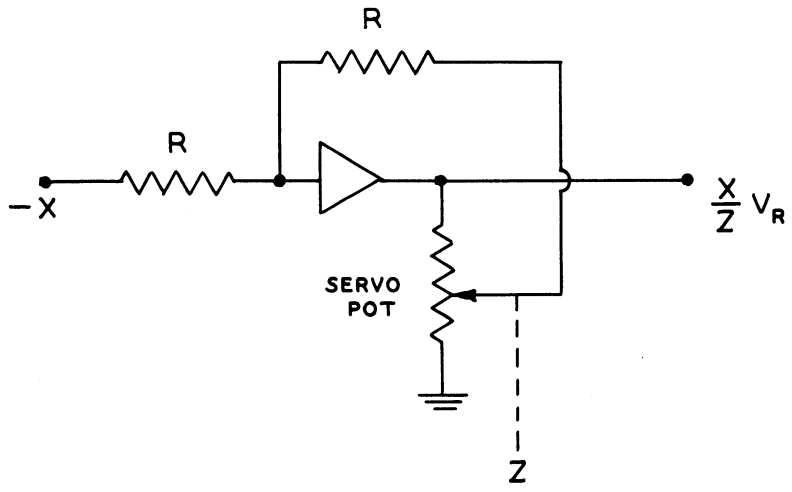

Figure III-5. Circuit for Division

III.3.3 Servo Function Generators

The servo multiplier described in the previous section can be utilized to multiply a voltage X by a function f (Z) of another voltage Z. This is accomplished by driving a potentiometer whose resistance does not vary linearly with wiper-arm position but instead varies as f (Z). A series of straight-line approximations to f (Z) can be obtained by connecting suitable padding resistors across tap connections along the potentiometer winding.

Servos for trigonometric resolution are actually special types of function generators. Here the resistance of a single-turn pot varies as the sine of the angle of shaft rotation θ. At $\theta = 0°$ and 180° the pot winding is grounded, while at $\theta = 90°$ and 270° the pot winding is connected to +V and -V volts respectively. The voltage at the wiper arm is then simply V sin θ. Another wiper arm displaced 90° from the first arm will have an output voltage V cos θ. The shaft angle θ is positioned in accordance with the servo input voltage.

APPENDIX IV

AUTOMATIC TESTING CIRCUITS

IV.1 Introduction

The use of automatic testing equipment for the computer section of flight simulators was discussed qualitatively in Section 3.3. The basic idea is to establish a given flight configuration as initial conditions on all of the integrators and to then check the output voltages of all amplifiers in the computer. Following this static check, the integrators are released and allowed to operate for some exactly preset length of time, after which the integrator outputs are held and checked against the values they should have. This latter test is a dynamic check.

IV.2 Circuit for Introducing Initial Conditions on Integrating Amplifiers

The output voltage of the integrating amplifier discussed in Section III.1.1 can be driven to any desired value by means of an initial-condition or reset relay, as shown for integrator number 1 at the top of Figure IV-1. The relay, when energized, disconnects the external input resistor or resistors from the dc amplifier input and instead connects the resistors R_{ci} and R_{c1} as input and feedback resistors respectively. The amplifier now has a static gain of R_{c1}/R_{ci} with an input of either plus or minus 100 volts. As a result, the static output voltage will be minus or plus 100 R_{c1}/R_{ci} volts respectively. By selecting R_{c1} and R_{ci} properly, the integrator output voltage can be made any desired value as long as the initial-condition relay is energized. When the relay is released the feedback capacitor C_1 is left with its charge of $\mp$ 100 R_{c1}/R_{ci} volts, the input resistor or resistors are reconnected to the dc amplifier input, and the integration proceeds.

Note that when the initial conditions are applied, the feedback capacitor C_1 prevents the new integrator output voltage from appearing instantaneously; instead the voltage builds up to its final value with a time constant of R_{c1} C_1 seconds.

IV.3 Circuit for Hold Operation of Integrating Amplifiers

In order to stop amplifiers from integrating it is necessary to disconnect the input resistor or resistors. This is accomplished on integrator

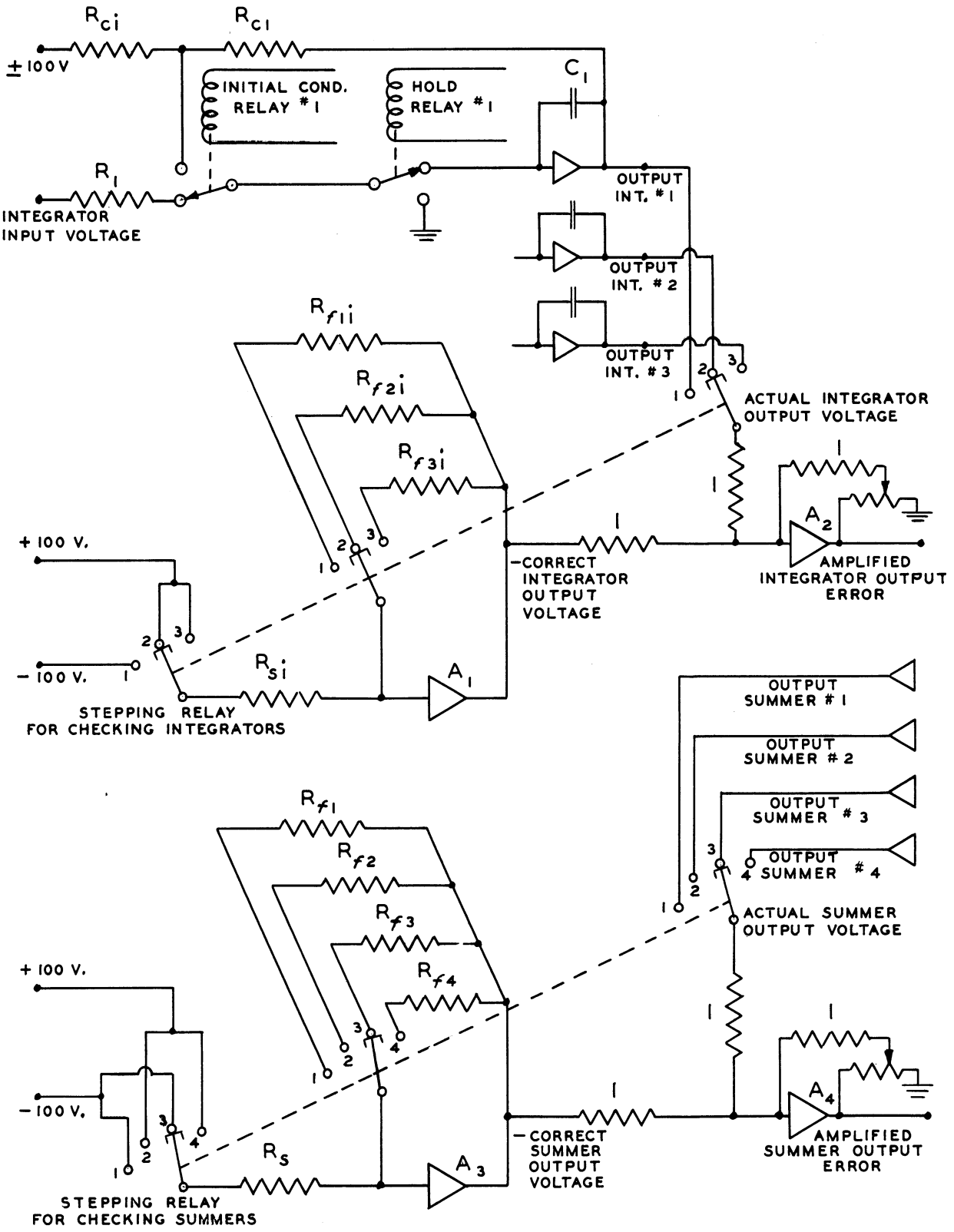

Figure IV-1. Schematic Diagram for Automatic Testing Circuit.

number 1 at the top of Figure IV-1 by energizing the hold relay. As soon as this is done the integrator output freezes at the voltage it had at that instant.

IV.4 Circuit for Automatic Testing

We have already seen how the initial-condition relays in Figure IV-1 can be used to set up any particular flight configuration in the simulator. One initial-condition relay and one pair of input and feedback resistors is necessary for each integrator in the computer section. While the integrator outputs are held at the proper initial voltages, the outputs of each of the summers are checked by means of the 3-gang stepping relay at the bottom of Figure IV-1. Amplifier A_3 is used to generate the correct output voltage for each successive summing amplifier. This is done by selecting with the first gang the proper polarity for the 100 volt input to A_3, and by selecting with the second gang the proper feedback resistor for A_3 to give the correct output voltage. On step 3, for example, the input to A_3 is -100 volts, and the output is then $+1.00\ R_{f3}/R_S$. This voltage, which represents the negative of the output which summer number 3 should have if it is operating properly, is compared with the actual output of summer number 3 by means of amplifier A_4. The output of A_4 then represents the amplified error of the output of summer number 3. This error can either be recorded as the stepping-relay automatically steps through all of its positions representing all of the summers, or it can be used through an auxiliary circuit to stop the relay on that step if the error is too large. It might also be worthwhile to include the output of the integrators in this test, just to check the voltages with their proper values for the given flight configuration.

For the dynamic test the initial-condition relays on the integrators are released for a preset length of time and the computer proceeds to solve the flight equations. The hold relays are then energized and the "frozen" output of each integrator is successively compared with the correct output voltage by means of the 3-gang stepping relay for checking integrators, shown in Figure IV-1. The operation of this relay, along with amplifiers A_1 and A_2, is identical with the stepping relay for checking the summers which was described in the previous paragraph. The amplified error of each integrator output appears as the output voltage of A_2. Again this can be recorded directly as the automatic stepping relay samples each integrator output, or it can be used to stop the relay on any step where the error is excessive.

The two automatic tests described above allow a quick static and dynamic quantitative check of the computer operation for a given flight condition. The tests could be mechanized for several other flight configurations if it were considered necessary or worthwhile.

APPENDIX V

ESTIMATED COST OF A COMPUTER SECTION BUILT FROM COMMERCIALLY AVAILABLE DC COMPONENTS

V.1 Cost of Computer Section Compared with the Entire Simulator

It seemed worthwhile for this report to make an estimate of the approximate cost of the simulator computer section if the computer were constructed entirely of commercially available dc electronic differential analyzer components. In comparing an estimate of this type with the current cost of simulators one must bear in mind several important factors. First of all, Special Devices Center has estimated that the cost of the entire computer section is only about 35% of the overall simulator cost; the rest of the cost estimates include housing 10%, cockpit 15%, instructors station 15%, radio aids 20%, and supplemental items 5%. Thus the cost estimates in this appendix are with respect to items covering only about one-third the cost of an entire trainer. Furthermore, the cost per simulator for engineering time in setting up the proper flight equations and computer circuits and configurations is considerable, particularly if only several simulators are built for one type of aircraft. With these thoughts in mind let us proceed with the computer-cost estimate.

V.2 Estimate of Number of Computer Components for a Typical Fighter Aircraft

In order to have a basis for a cost estimate, it is of course necessary to consider the number of summing amplifiers, scale-setting potentiometers, integrating amplifiers, servo multipliers, servo function generators, and servo resolvers. The estimates for a typical fighter aircraft are shown below:

Summing amplifiers	62
Integrating Amplifiers	16
Scale-setting potentiometer	70
Servos for multiplication, function generation, and resolution	18

Almost all the servos must drive more than one potentiometer; the maximum number of pots are required for the Mach number servo.

V.3 Cost Estimate for Commercial DC Equipment

As a basis for the cost estimate if commercial dc electronic differential analyzer equipment is utilized, we have employed the components of Electronic Associates, Inc., as a yardstick. This does not imply that we feel this equipment is necessarily the best, but the Electronic Associates servos are fairly similar to ones which might be employed in a flight simulator and we happen to have rough cost figures available for their equipment. The cost estimates, if based on other computer manufacturers equipment, would be comparable. The breakdown is as follows:

Summing and integrating amplifiers four 20-amplifier racks at $12,500	$50,000
Servos for multiplication function generation, and resolution one 20-servo rack at $25,000	$25,000
80-amplifier console including potentiometers and computing resistors and integrators	$25,000
Approximate total Estimated cost	$100,000

In the above estimate we have assumed that small one-turn 1% resolving pots are used instead of the standard Electronic Associates high-precision resolvers. One should note that centrally located power supplies, elimination of drift-stabilized amplifiers and other items should cut the above estimates very considerably. On the other hand, engineering and other additional costs would raise the figure. Hence we feel that this very rough estimate is about indicative of the cost of a computer section if fabricated from commercially available dc computer components.